

Recurrence relations for the generalized Laguerre and Charlier orthogonal polynomials and discrete Painlevé equations on the $D_6^{(1)}$ Sakai surface

Xing Li

Department of Mathematics, Shanghai University, Shanghai 200444, P.R.China

E-mail: xing26@shu.edu.cn

Anton Dzhamay

School of Mathematical Sciences, The University of Northern Colorado, Greeley, CO 80639, USA

E-mail: anton.dzhamay@unco.edu

Galina Filipuk

Institute of Mathematics, Faculty of Mathematics, Informatics and Mechanics, University of Warsaw, Banacha 2, Warsaw, 02-097, Poland

E-mail: filipuk@mimuw.edu.pl

Da-jun Zhang

Department of Mathematics, Shanghai University, Shanghai 200444, P.R.China

E-mail: djzhang@staff.shu.edu.cn

Keywords: orthogonal polynomials, Askey-Wilson scheme, Painlevé equations, difference equations, birational transformations.

MSC2010: 33C47, 34M55, 39A99, 42C05, 3D45, 34M55, 34M56, 14E07, 39A13

Abstract

In this paper we consider two examples of certain recurrence relations, or nonlinear discrete dynamical systems, that appear in the theory of orthogonal polynomials, from the point of view of Sakai's geometric theory of Painlevé equations. On one hand, this gives us new examples of the appearance of discrete Painlevé equations in the theory of orthogonal polynomials. On the other hand, it serves as a good illustration of the effectiveness of a recently proposed procedure on how to reduce such recurrences to some canonical discrete Painlevé equations. Of particular interest is the fact that both recurrences are regularized on the same family of rational algebraic surfaces, but at the same time their dynamics are non-equivalent.

1 Introduction

It is well known that Painlevé equations, both differential and discrete, often appear in the study of various orthogonal polynomial ensembles, see for example a recent monograph of Walter Van Assche, [VA18]. For example, discrete Painlevé equations describe the dependence of the coefficients of the *three-term recurrence relations* and *ladder operators* as functions of the degree variable n , whereas differential Painlevé equations sometimes describe their dependence on some continuous weight parameters. This relationship is due

to a connection between orthogonal polynomial ensembles and certain isomonodromy problems, as explained in a series of recent papers by Alexei Borodin and his collaborators. The main reference here is [BB03], see also [AB06, AB09, Bor03]. However, in practice it is often quite difficult to recognize exactly which Painlevé equations appear. And even when we have some problem-specific information that suggests the type of the corresponding Painlevé equations, finding explicit reduction to some canonical form is a highly non-obvious task. In a recent paper [DFS20] two of the authors, together with Alexander Stokes, suggested an explicit step-by-step procedure of reducing discrete Painlevé equations that appear in applied problems to their standard form by finding some appropriate change of coordinates. This procedure is based on the geometric theory of discrete Painlevé equations created by Hidetaka Sakai [Sak01], see also an important recent survey paper [KNY17]. In general, Sakai's geometric theory seems to be a very natural framework for this kind of problems. And to better understand the relationship between various weights for orthogonal polynomials and discrete Painlevé equations it is important to have a large collection of explicit examples.

Another interesting aspect of this problem is that, in addition to the geometric classification of discrete Painlevé equations by the type of the rational algebraic surface on which the equation is regularized, there is a finer classification by the conjugacy class of the translation element in the extended affine Weyl symmetry group of the surface, where this translation element defined the actual dynamic. Thus, there are infinitely many non-equivalent discrete Painlevé equations, and it is interesting to see which of those equations appear in applied problems, especially among the natural simple equations corresponding to short translations in the symmetry sub-lattice.

In this paper we consider two examples of nonlinear recurrence relations from the theory of orthogonal polynomials that reduce to discrete Painlevé equations. The first recurrence describes the coefficients of ladder operators for a certain generalization of Laguerre orthogonal polynomials, and the second describes the coefficients of the three-term recurrence relation for generalized Charlier polynomials. Both recurrences get regularized on a rational algebraic surfaces of type $D_6^{(1)}$, but the resulting translations are *non-equivalent*. In fact, the first recurrence corresponds to discrete Painlevé equation given by equation (8.29) in Section 8.1.20 in [KNY17] (equation (38) in Appendix A), and the second to the so-called alt. d- P_{II} equation in [Sak01] (equation (44) in Appendix A). Based on the translations these equations define, we denote them by $[1\bar{1}\bar{1}1]$ and by $[00\bar{1}1]$ respectively.

Thus, we see the importance of understanding not just the type of the surface, but also the actual translation element. Further, the geometric approach allows us to quickly and completely understand each dynamic, decompose it as a composition of elementary Bäcklund transformations, and also match the parameters of the weight with the canonical Painlevé parameters.

The paper is organized as follows. In Section 2 we give a rather detailed step-by-step illustration on how to use the geometric tools of the Sakai theory to solve the Painlevé identification problem for the generalized Laguerre weight example. In Section 3 we give a very brief summary of the identification for the generalized Charlier example. We collect some of the standard algebro-geometric data for the $D_6^{(1)}$ surface in Appendix A.

2 Generalized Laguerre Weight and the MacDonalD Hierarchy

In this section we consider an example of a recurrence relation on the coefficients of ladder operators that appeared in a paper [CI10] by Yang Chen and Alexander Its, who studied a certain linear statistics for the *unitary Laguerre ensemble*. That statistics can in turn be interpreted as a singular perturbation of the standard Laguerre weight $x^\alpha e^{-s}$ by a multiplicative factor $e^{-s/x}$ that induces an infinitely strong zero at the origin. This perturbed Laguerre weight was further considered in [CC15, CFR19, XDZ15] (see also the references therein).

The setup is as follows. Consider a collection of monic polynomials $\{P_n(x) = x^n + p_1(n)x^{n-1} + \dots + P_n(0)\}$ orthogonal with respect to the weight $w(x) = w(x; \alpha, s)$, depending on two parameters $\alpha > 0, s > 0$ (we often omit the explicit dependence of parameters or include only the relevant one, usually s , in the formulae below):

$$\int_0^\infty P_j(x)P_k(x)w(x; \alpha, s) dx = h_j(\alpha, s)\delta_{jk}, \quad w(x; \alpha, s) = x^\alpha e^{-s} e^{-s/x}, \\ 0 \leq x < \infty, \quad \alpha > 0, s > 0.$$

Orthogonal polynomials satisfy a three-term recurrence relation

$$xP_n(x) = P_{n+1}(x) + \alpha_n P_n(x) + \beta_n P_{n-1}(x), \quad (1)$$

where $\alpha_n \in \mathbb{R}$ and $\beta_n = h_n/h_{n-1}$. One can also define the so-called *ladder operators*

$$\left(\frac{d}{dx} + B_n(x)\right) P_n(x) = \beta_n A_n(x) P_{n-1}(x), \\ \left(\frac{d}{dx} - B_n(x) - v'(x)\right) P_{n-1}(x) = -A_{n-1}(x) P_n(x), \quad v(x) := -\ln w(x),$$

satisfying the fundamental compatibility conditions

$$B_{n+1}(x) + B_n(x) = (x - \alpha_n)A_n(x) - v'(x), \\ 1 + (x - \alpha_n)(B_{n+1}(x) - B_n(x)) = \beta_{n+1}A_{n+1}(x) - \beta_n A_{n-1}(x).$$

In this particular case the ladder operators can be parameterized by some variables a_n and b_n as follows:

$$A_n(x) = \frac{1}{x} + \frac{a_n}{x^2}, \quad a_n(s) = \frac{s}{h_n} \int_0^\infty \frac{P_n^2(x)}{x} w(x) dx, \\ B_n(x) = -\frac{n}{x} + \frac{b_n}{x^2}, \quad b_n(s) = \frac{s}{h_{n-1}} \int_0^\infty \frac{P_n(x)P_{n-1}(x)}{x} w(x) dx.$$

These variables satisfy the recurrence relation

$$b_n + b_{n+1} = s - (2n + 1 + \alpha + a_n)a_n, \\ (b_n^2 - sb_n)(a_n + a_{n-1}) = [ns - (2n + \alpha)b_n]a_n a_{n-1}, \quad (2)$$

which is the recurrence relation that we study. For the orthogonal polynomial ensemble under consideration the initial conditions for this recurrence are given by

$$a_0(s) = \sqrt{s} \frac{K_\alpha(2\sqrt{s})}{K_{\alpha+1}(2\sqrt{s})}, \quad b_0(s) = 0,$$

where $K_\alpha(z)$ is the MacDonald function (the modified Bessel function) of the second kind, and for this reason this recurrence is called the MacDonald hierarchy in [CI10]. Note that it is also possible to explicitly express the coefficients α_n and β_n of the three-term recurrence relation in terms of variables a_n and b_n ,

$$\alpha_n = 2n + 1 + \alpha + a_n, \quad \beta_n a_n^2 = [ns - (2n + \alpha)b_n]a_n - (b_n^2 - sb_n).$$

Another important objects associated with the weight $w(x; \alpha, s)$ are the determinant $D_n(s)$ of its moment matrix, also known as the *Hankel determinant*, and its logarithmic derivative $H_n(s)$,

$$D_n(s) = \det \left[\int_0^\infty x^{j+k} x^\alpha e^{-x-s/x} \right]_{j,k=0}^{n-1} = \prod_{j=0}^{n-1} h_j(\alpha, s), \quad H_n(s) := s \frac{d}{ds} \ln D_n(s). \quad (3)$$

As shown in [CI10], the quantities a_n and b_n (and hence α_n and β_n) can be written in terms of this logarithmic derivative as follows:

$$\begin{aligned} a_n &= H_n - H_{n+1}, \\ b_n &= \frac{ns + \delta^2 H_n [H_n - n(n + \alpha)]}{2n + \alpha + \delta^2 H_n}, \quad \text{where } \delta^2 H_n := H_{n-1} - H_{n+1} = a_n + a_{n-1}. \end{aligned} \quad (4)$$

Substituting the above into (2) results

$$\begin{aligned} &\{[H_n - n(n + \alpha)]\delta^2 H_n + ns\} \{[H_n - n(n + \alpha) - s]\delta^2 H_n - (n + \alpha)s\} \\ &= (2n + \alpha + \delta^2 H_n) \{ns + (2n + \alpha)[n(n + \alpha) - H_n]\} (H_n - H_{n+1})(H_{n-1} - H_n). \end{aligned} \quad (5)$$

It is not difficult to show that conversely, equation (5) is equivalent to recurrence relations (2).

In [CI10] Chen and Its gave the Lax Pair for equation (5), and so this is an integrable discrete equation. Moreover, in [CI10, CFR19] it has been argued that it can be obtained as some composition of elementary Bäcklund-Schlesinger transformation of the (generic) third Painlevé equation, and hence it should be one of discrete Painlevé equations on the $D_6^{(1)}$ Sakai surface. However, an explicit identification with one of the standard discrete Painlevé equations was not provided. In this section we show that (2) is indeed equivalent to the standard d-P $(2A_1^{(1)}/D_6^{(1)})$ equation as written in [KNY17]. However, we first change the notation from a_n and b_n to x_n and y_n to avoid clashing with the standard notation for root

variables in the geometric Painlevé theory. Thus, our main object of study is the following discrete dynamical system:

$$\begin{cases} (x_n + x_{n-1})(y_n^2 - sy_n) = (ns - (2n + \alpha)y_n)x_nx_{n-1}, \\ y_n + y_{n+1} = s - (2n + 1 + \alpha + x_n)x_n. \end{cases} \quad (6)$$

Our main result is the explicit change of variables and parameter identification establishing the above equivalence that is given in the following Theorem.

Theorem 1. *Recurrence (6) is equivalent to the standard d - $P(2A_1^{(1)}/D_6^{(1)})$ equation (38) via the following explicit change of coordinates and parameter identification (here a_i denote the root variables, or the canonical parameters for a discrete Painlevé equation, see Section 2.4)*

$$\begin{cases} x(q, p) = \frac{t}{q}, \\ y(q, p) = -pt - \frac{t(a_2 - a_0)}{q} - \frac{t^2}{q^2}, \\ n = 1 - a_1 = -a_0, \\ \alpha = a_2 - a_1, s = -t, \end{cases} \quad \begin{cases} q(x, y) = -\frac{s}{x}, \\ p(x, y) = \frac{x^2 + x(1 + 2n + \alpha) + y}{s}, \\ a_0 = -n, a_1 = 1 + n, \\ a_2 = 1 + n + \alpha, a_3 = -n - \alpha, t = -s. \end{cases} \quad (7)$$

We now give a detailed proof of this theorem following the algorithmic approach of [DFS20].

2.1 The singularity structure of the recurrence relation

Recurrence (6) defines two half-step mappings, the *forward half-mapping*

$$\tilde{\varphi}_1^n : (x_n, y_n) \mapsto (x_n, y_{n+1}) = (x_n, s - y_n - x_n(1 + 2n + x_n + \alpha)), \quad (8)$$

and the *backward half-mapping*

$$\tilde{\varphi}_2^n : (x_n, y_n) \mapsto (x_{n-1}, y_n) = \left(\frac{x_n y_n (y_n - s)}{n x_n (s - 2y_n) - y_n (\alpha x_n + y_n - s)}, y_n \right). \quad (9)$$

The first step of the process is to extend the mapping from $\mathbb{C} \times \mathbb{C}$ to $\mathbb{P}^1 \times \mathbb{P}^1$ by introducing three additional charts (X, y) , (x, Y) , and (X, Y) , where $X = 1/x$, $Y = 1/y$, and then to find the *base points* of the mapping where the numerator and the denominator of rational functions defining the mapping simultaneously vanish. It is also convenient to omit the index n by introducing the standard notation $x := x_n$, $\bar{x} := x_{n+1}$, $\underline{x} := x_{n-1}$, and similarly for y .

Looking at the backward half-mapping in the (x, y) -chart,

$$\tilde{\varphi}_2 : (x, y) \mapsto (\underline{x}, y) = \left(\frac{xy(y - s)}{nx(s - 2y) - y(\alpha x + y - s)}, y \right),$$

we immediately see two base points, $q_1(0, 0)$ and $q_3(0, s)$ (the reason for the choice for indices will be clear once we find all of the base points) for the mapping $\underline{x} = \underline{x}(x, y)$. To resolve

the indeterminacy of the mapping, for each base point $q_i(x_i, y_i)$ we introduce two new local coordinate charts (u_i, v_i) and (U_i, V_i) by

$$x = x_i + u_i = x_i + U_i V_i, \quad y = y_i + u_i v_i = y_i + V_i.$$

This is known as the *blowup procedure* in algebraic geometry, see standard textbooks [Sha13, GH78] (or [DFS20] for a brief summary sufficient for our purposes). This procedure modifies the geometry of the domain (and hence the range) of the mapping by gluing an *exceptional divisor* $F_i \simeq \mathbb{P}^1$ in place of q_i . Locally, in (u_1, v_1) (resp. (U_1, V_1)) chart F_i is given by the equation $u_i = 0$ (resp. $V_i = 0$) and is parameterized by v_i (resp. U_i) with $U_i = 1/v_i$. We then need to extend the mapping to F_i via coordinate substitution and then check to see whether there are any new base points on F_i .

In particular, after the substitution $(x, y) = (u_1, u_1 v_1)$ the expression for \underline{x} becomes

$$\underline{x}(u_1, v_1) = \frac{u_1 v_1 (s - u_1 v_1)}{v_1 (u_1 (\alpha + 2n + v_1) - s) - n s},$$

and so we see a new base point $q_2(u_1 = 0, v_1 = -n)$. Performing a similar computation in the (U_1, V_1) chart and then in new (u_2, v_2) and (U_2, V_2) charts gives no new base points for the whole backward half-mapping $\tilde{\varphi}_2$ and the mapping in these charts is now well-defined everywhere. We call this configuration of base points

$$q_1(x = 0, y = 0) \leftarrow q_2(u_1 = 0, v_1 = -n)$$

a *degeneration cascade* resolving the base point q_1 . We get a similar degeneration cascade resolving the point q_3

$$q_3(x = 0, y = s) \leftarrow q_4(u_3 = 0, v_3 = -n - \alpha).$$

There are no more singular points for the backward half-mapping, but for the forward half-mapping $\tilde{\varphi}_1$, when considered in the (X, Y) chart, we get another cascade of base points,

$$\begin{aligned} q_5(X = 0, Y = 0) &\leftarrow q_6(u_5 = X = 0, v_5 = xY = 0) \leftarrow q_7(u_6 = X, v_6 = x^2 Y = -1) \\ &\leftarrow q_8(u_7 = X, v_7 = x(1 + x^2 Y) = 1 + 2n + \alpha). \end{aligned}$$

Blowing up all 8 points q_i gives us a (family of) rational algebraic surfaces parameterized by n, α, s (coordinates of the base points); $\mathcal{X} = \mathcal{X}_{n, \alpha, s}$. An important object associated with this family is the *Picard lattice*

$$\text{Pic}(\mathcal{X}) = \text{Span}_{\mathbb{Z}}\{\mathcal{H}_x, \mathcal{H}_y, \mathcal{F}_1, \dots, \mathcal{F}_8\} \simeq \text{Cl}(\mathcal{X})$$

generated by the classes $\mathcal{H}_{x,y} = [H_{x,y=k}]$ of coordinate lines and classes $\mathcal{F}_i = [F_i]$ of the exceptional divisors. $\text{Pic}(\mathcal{X})$ is equipped with the symmetric bilinear *intersection form* given by

$$\mathcal{H}_x \bullet \mathcal{H}_x = \mathcal{H}_y \bullet \mathcal{H}_y = \mathcal{H}_x \bullet \mathcal{F}_i = \mathcal{H}_y \bullet \mathcal{F}_j = 0, \quad \mathcal{H}_x \bullet \mathcal{H}_y = 1, \quad \mathcal{F}_i \bullet \mathcal{F}_j = -\delta_{ij} \quad (10)$$

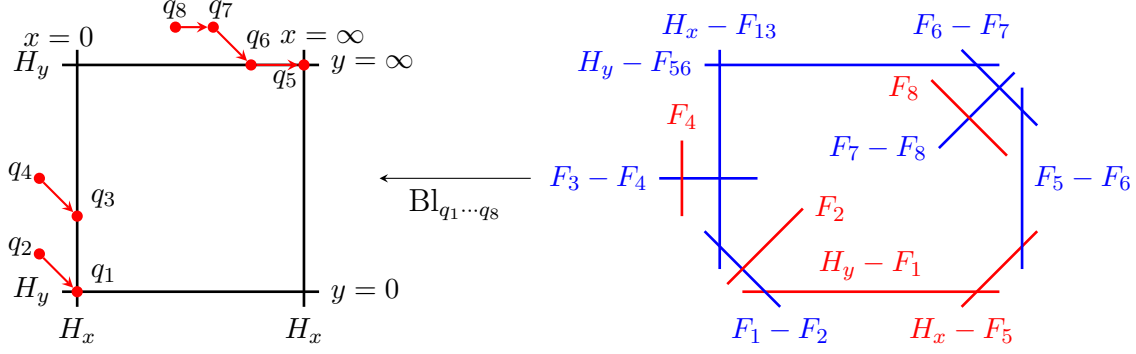


Figure 1: The Sakai Surface for the generalized Laguerre recurrence

on the generators, and then extended by linearity.

This configuration of the base points and the rational algebraic surface \mathcal{X} obtained after we do all eight blowups are shown on Figure 1. We also mark on the surface \mathcal{X} a number of special curves, such as the exceptional divisors F_i and some other curves with the self-intersection -1 and -2 .

It is easy to see that this configuration of the blowup points lies on a (reducible) bi-quadratic curve given by the equation $x^2 = 0$ in the affine (x, y) -chart. This curve is the polar divisor of a symplectic form $\omega = (k/x^2)dx \wedge dy$ and the class of the divisor of this symplectic form $[\omega]$ in the *Picard lattice* is called the *canonical* divisor class, $\mathcal{K}_{\mathbb{P}^1 \times \mathbb{P}^1}$. We are interested in the dual, or *anti-canonical*, divisor class of the lift of ω to the surface \mathcal{X} :

$$-\mathcal{K}_{\mathcal{X}} = -[K_{\mathcal{X}}] = 2\mathcal{H}_x + 2\mathcal{H}_y - \mathcal{F}_1 - \dots - \mathcal{F}_8 = \delta_0 + \delta_1 + 2\delta_2 + 2\delta_3 + 2\delta_4 + \delta_5 + \delta_6, \quad (11)$$

where $\delta_i = [d_i]$ are classes of the *irreducible components* of the anti-canonical divisor $K_{\mathcal{X}}$ shown on Figure 2. The irreducible components d_i are -2 curves that are shown on Figure 1 on the right. Elements $\delta_i \in \text{Pic}(\mathcal{X})$ constitute the *surface root basis* of the surface family

$$\begin{array}{ccc}
 \delta_0 \circ & & \delta_6 \circ \\
 & \diagdown & / \\
 & \delta_2 \circ & \delta_4 \circ \\
 & / & \diagdown \\
 \delta_1 \circ & & \delta_5 \circ
 \end{array}
 \quad
 \begin{array}{ll}
 \delta_0 = \mathcal{F}_1 - \mathcal{F}_2, & \delta_4 = \mathcal{F}_6 - \mathcal{F}_7, \\
 \delta_1 = \mathcal{F}_3 - \mathcal{F}_4, & \delta_5 = \mathcal{F}_5 - \mathcal{F}_6, \\
 \delta_2 = \mathcal{H}_x - \mathcal{F}_{13}, & \delta_6 = \mathcal{F}_7 - \mathcal{F}_8, \\
 \delta_3 = \mathcal{H}_y - \mathcal{F}_{56}, &
 \end{array}
 \quad (12)$$

Figure 2: The (preliminary) Surface Root Basis for the generalized Laguerre recurrence

$\mathcal{X}_{n,\alpha,s}$ and their intersection configuration is encoded in an affine Dynkin diagram shown on Figure 2. This diagram has the type $D_6^{(1)}$ and so we expect that our recurrence is given by a discrete Painlevé equation in this family. In Appendix A we collect some essential algebro-geometric facts about discrete Painlevé equations of surface type $D_6^{(1)}$. It now remains to

determine which discrete Painlevé equation our dynamic corresponds to. For that, we need to look at the induced mapping on the Picard lattice, and associated action on the surface and symmetry root bases, we do that next.

2.2 Induced linear mappings on the Picard lattice

We now compute the linearized action on the Picard lattice for the half-maps $\tilde{\varphi}_1, \tilde{\varphi}_2$, as well as the full *forward map* $\tilde{\varphi}_n = (\tilde{\varphi}_2^{n+1})^{-1} \circ \tilde{\varphi}_1^n : (x_n, y_n) \rightarrow (x_{n+1}, y_{n+1})$ (that we write simply as $\tilde{\varphi} : (x, y) \rightarrow (\bar{x}, \bar{y})$) and the full *backward map* $\tilde{\varphi}^{-1} : (x, y) \rightarrow (\underline{x}, \underline{y})$. This computation is standard and is explained in detail, for example, in [DFS20, DT18], so here we only state the result. Note that sometimes it is convenient to abbreviate $\mathcal{F}_{i_1} + \mathcal{F}_{i_2} + \dots + \mathcal{F}_{i_k}$ as $\mathcal{F}_{i_1 i_2 \dots i_k}$.

Lemma 2.

(a) *The action of the half-step forward dynamic $(\tilde{\varphi}_1)_* : \text{Pic}(\mathcal{X}) \rightarrow \text{Pic}(\bar{\mathcal{X}})$ is given by*

$$\begin{aligned} \mathcal{H}_x &\mapsto \bar{\mathcal{H}}_x, & \mathcal{F}_4 &\mapsto \bar{\mathcal{F}}_2, \\ \mathcal{H}_y &\mapsto 2\bar{\mathcal{H}}_x + \bar{\mathcal{H}}_y - \bar{\mathcal{F}}_{5678}, & \mathcal{F}_5 &\mapsto \bar{\mathcal{H}}_x - \bar{\mathcal{F}}_8, \\ \mathcal{F}_1 &\mapsto \bar{\mathcal{F}}_3, & \mathcal{F}_6 &\mapsto \bar{\mathcal{H}}_x - \bar{\mathcal{F}}_7, \\ \mathcal{F}_2 &\mapsto \bar{\mathcal{F}}_4, & \mathcal{F}_7 &\mapsto \bar{\mathcal{H}}_x - \bar{\mathcal{F}}_6, \\ \mathcal{F}_3 &\mapsto \bar{\mathcal{F}}_1, & \mathcal{F}_8 &\mapsto \bar{\mathcal{H}}_x - \bar{\mathcal{F}}_5. \end{aligned}$$

Under this mapping points q_2 and q_4 evolve as if $n \mapsto n + 1$ and as a result we get $\bar{q}_2(0, -n - 1), \bar{q}_4(0, -n - 1 - \alpha)$, but all of the other points do not evolve.

(b) *The action of the half-step backward dynamic $(\tilde{\varphi}_2)_* : \text{Pic}(\mathcal{X}) \rightarrow \text{Pic}(\underline{\mathcal{X}})$ is given by*

$$\begin{aligned} \mathcal{H}_x &\mapsto \underline{\mathcal{H}}_x + 2\underline{\mathcal{H}}_y - \underline{\mathcal{F}}_{1234}, & \mathcal{F}_4 &\mapsto \underline{\mathcal{H}}_y - \underline{\mathcal{F}}_3, \\ \mathcal{H}_y &\mapsto \underline{\mathcal{H}}_y, & \mathcal{F}_5 &\mapsto \underline{\mathcal{F}}_5, \\ \mathcal{F}_1 &\mapsto \underline{\mathcal{H}}_y - \underline{\mathcal{F}}_2, & \mathcal{F}_6 &\mapsto \underline{\mathcal{F}}_6, \\ \mathcal{F}_2 &\mapsto \underline{\mathcal{H}}_y - \underline{\mathcal{F}}_1, & \mathcal{F}_7 &\mapsto \underline{\mathcal{F}}_7, \\ \mathcal{F}_3 &\mapsto \underline{\mathcal{H}}_y - \underline{\mathcal{F}}_4, & \mathcal{F}_8 &\mapsto \underline{\mathcal{F}}_8. \end{aligned}$$

Under this mapping the point q_8 evolves as if $n \mapsto n - 1$ and we get $\underline{q}_8(0, -1 + 2n + \alpha)$. All the other points do not evolve.

(c) *The action of the full forward dynamic $(\tilde{\varphi})_* : \text{Pic}(\mathcal{X}) \rightarrow \text{Pic}(\bar{\mathcal{X}})$ is given by*

$$\begin{aligned} \mathcal{H}_x &\mapsto \bar{\mathcal{H}}_x + 2\bar{\mathcal{H}}_y - \bar{\mathcal{F}}_{1234}, & \mathcal{F}_4 &\mapsto \bar{\mathcal{H}}_y - \bar{\mathcal{F}}_1, \\ \mathcal{H}_y &\mapsto 2\bar{\mathcal{H}}_x + 5\bar{\mathcal{H}}_y - 2\bar{\mathcal{F}}_{1234} - \bar{\mathcal{F}}_{5678}, & \mathcal{F}_5 &\mapsto \bar{\mathcal{H}}_x + 2\bar{\mathcal{H}}_y - \bar{\mathcal{F}}_{12348}, \\ \mathcal{F}_1 &\mapsto \bar{\mathcal{H}}_y - \bar{\mathcal{F}}_4, & \mathcal{F}_6 &\mapsto \bar{\mathcal{H}}_x + 2\bar{\mathcal{H}}_y - \bar{\mathcal{F}}_{12347}, \\ \mathcal{F}_2 &\mapsto \bar{\mathcal{H}}_y - \bar{\mathcal{F}}_3, & \mathcal{F}_7 &\mapsto \bar{\mathcal{H}}_x + 2\bar{\mathcal{H}}_y - \bar{\mathcal{F}}_{12346}, \\ \mathcal{F}_3 &\mapsto \bar{\mathcal{H}}_y - \bar{\mathcal{F}}_2, & \mathcal{F}_8 &\mapsto \bar{\mathcal{H}}_x + 2\bar{\mathcal{H}}_y - \bar{\mathcal{F}}_{12345}. \end{aligned}$$

Under this mapping we get the expected evolution of the discrete parameter $n \mapsto n + 1$, so we get $\bar{q}_2(0, -n - 1)$, $\bar{q}_4(0, -n - 1 - \alpha)$, and $\bar{q}_8(0, 3 + 2n + \alpha)$.

(d) The action of the full backward dynamic $(\bar{\varphi})_*^{-1} : \text{Pic}(\mathcal{X}) \rightarrow \text{Pic}(\underline{\mathcal{X}})$ is given by

$$\begin{aligned} \mathcal{H}_x &\mapsto 5\underline{\mathcal{H}}_x + 2\underline{\mathcal{H}}_y - \underline{\mathcal{F}}_{1234} - 2\underline{\mathcal{F}}_{5678}, & \mathcal{F}_4 &\mapsto 2\underline{\mathcal{H}}_x + \underline{\mathcal{H}}_y - \underline{\mathcal{F}}_{15678}, \\ \mathcal{H}_y &\mapsto 2\underline{\mathcal{H}}_x + \underline{\mathcal{H}}_y - \underline{\mathcal{F}}_{5678}, & \mathcal{F}_5 &\mapsto \underline{\mathcal{H}}_x - \underline{\mathcal{F}}_8, \\ \mathcal{F}_1 &\mapsto 2\underline{\mathcal{H}}_x + \underline{\mathcal{H}}_y - \underline{\mathcal{F}}_{45678}, & \mathcal{F}_6 &\mapsto \underline{\mathcal{H}}_x - \underline{\mathcal{F}}_7, \\ \mathcal{F}_2 &\mapsto 2\underline{\mathcal{H}}_x + \underline{\mathcal{H}}_y - \underline{\mathcal{F}}_{35678}, & \mathcal{F}_7 &\mapsto \underline{\mathcal{H}}_x - \underline{\mathcal{F}}_6, \\ \mathcal{F}_3 &\mapsto 2\underline{\mathcal{H}}_x + \underline{\mathcal{H}}_y - \underline{\mathcal{F}}_{25678}, & \mathcal{F}_8 &\mapsto \underline{\mathcal{H}}_x - \underline{\mathcal{F}}_5. \end{aligned}$$

Under this mapping we get the expected evolution of the discrete parameter $n \mapsto n - 1$, so we get $\underline{q}_2(0, -n + 1)$, $\underline{q}_4(0, -n + 1 - \alpha)$, and $\underline{q}_8(0, -1 + 2n + \alpha)$.

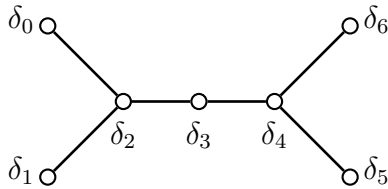
Remark 3. It may seem strange that for half-maps in (a) and (b) some base points evolve as if n evolves, but some do not, this does not happen for full maps. The reason for that is that for half-maps the evolution on the Picard lattice is not a translation, and so root variables (and hence the parameters of the base points) evolve in a more complicated fashion. We briefly explain that in Section 2.6.

2.3 Identifying the dynamics on the level of the Picard lattice

We are now in the position to start identifying the dynamic. For that, we first need to find some change of basis of the Picard lattice that matches the corresponding surface and symmetry root bases. As usual, we begin with the preliminary change of basis that identifies the symmetry roots. It is given in the next Lemma.

Lemma 4. *The change of basis identifying the surface roots corresponding to the irreducible components of the anti-canonical divisors for the standard surface on Figure 6 and the Sakai surface we obtained regularizing the generalized Laguerre recurrence on Figure 1 is very natural and is given by $\mathcal{H}_x = \mathcal{H}_q$, $\mathcal{H}_y = \mathcal{H}_p$, and $\mathcal{F}_i = \mathcal{E}_i$.*

Proof. This change of basis follows immediately when we compare the root bases on Figures 2 and 5:



$$\begin{aligned} \delta_0 &= \mathcal{E}_1 - \mathcal{E}_2 = \mathcal{F}_1 - \mathcal{F}_2, & \delta_4 &= \mathcal{E}_6 - \mathcal{E}_7 = \mathcal{F}_6 - \mathcal{F}_7, \\ \delta_1 &= \mathcal{E}_3 - \mathcal{E}_4 = \mathcal{F}_3 - \mathcal{F}_4, & \delta_5 &= \mathcal{E}_5 - \mathcal{E}_6 = \mathcal{F}_5 - \mathcal{F}_6, \\ \delta_2 &= \mathcal{H}_q - \mathcal{E}_{13} = \mathcal{H}_x - \mathcal{F}_{13}, & \delta_6 &= \mathcal{E}_7 - \mathcal{E}_8 = \mathcal{F}_7 - \mathcal{F}_8, \\ \delta_3 &= \mathcal{H}_p - \mathcal{E}_{56} = \mathcal{H}_y - \mathcal{F}_{56}, \end{aligned}$$

□

With this identification we get the symmetry root basis for the Laguerre recurrence to be

$$\alpha_0 = 2\mathcal{H}_x + \mathcal{H}_y - \mathcal{F}_{345678}, \quad \alpha_1 = \mathcal{H}_y - \mathcal{F}_{12}, \quad \alpha_2 = \mathcal{H}_y - \mathcal{F}_{34}, \quad \alpha_3 = 2\mathcal{H}_x + \mathcal{H}_y - \mathcal{F}_{125678},$$

and the full forward evolution $(\tilde{\varphi})_*$ from Lemma 2(c) acts on the symmetry roots as

$$\tilde{\varphi}_* : \alpha = \langle \alpha_0, \alpha_1, \alpha_2, \alpha_3 \rangle \mapsto \tilde{\varphi}_*(\alpha) = \alpha + \langle -1, 1, 1, -1 \rangle \delta,$$

which is the *opposite* of the standard translation (40). To *reverse* the translation direction we can act on the symmetry roots by the Dynkin diagram automorphisms σ_i described in Section A.2 as follows:

$$\sigma_2 \circ \sigma_1 \circ \sigma_2 \circ \sigma_1 = (\alpha_0 \alpha_1)(\alpha_0 \alpha_3)(\alpha_1 \alpha_2)(\alpha_0 \alpha_1)(\alpha_0 \alpha_3)(\alpha_1 \alpha_2) = (\alpha_0 \alpha_1)(\alpha_2 \alpha_3).$$

This action then adjusts our change of basis and this results in the correct change of basis given in the following Lemma.

Lemma 5. *The change of basis of the Picard lattice identifying both the geometry and the standard dynamics between the Laguerre recursion and the standard discrete Painlevé dynamics (42) is given by:*

$$\begin{aligned} \mathcal{H}_x &= \mathcal{H}_q, & \mathcal{H}_q &= \mathcal{H}_x, \\ \mathcal{H}_y &= 2\mathcal{H}_q + \mathcal{H}_p - \mathcal{E}_{5678}, & \mathcal{H}_p &= 2\mathcal{H}_x + \mathcal{H}_y - \mathcal{F}_{5678}, \\ \mathcal{F}_1 &= \mathcal{E}_3, & \mathcal{E}_1 &= \mathcal{F}_3, \\ \mathcal{F}_2 &= \mathcal{E}_4, & \mathcal{E}_2 &= \mathcal{F}_4, \\ \mathcal{F}_3 &= \mathcal{E}_1, & \mathcal{E}_3 &= \mathcal{F}_1, \\ \mathcal{F}_4 &= \mathcal{E}_2, & \mathcal{E}_4 &= \mathcal{F}_2, \\ \mathcal{F}_5 &= \mathcal{H}_q - \mathcal{E}_8, & \mathcal{E}_5 &= \mathcal{H}_x - \mathcal{F}_8, \\ \mathcal{F}_6 &= \mathcal{H}_q - \mathcal{E}_7, & \mathcal{E}_6 &= \mathcal{H}_x - \mathcal{F}_7, \\ \mathcal{F}_7 &= \mathcal{H}_q - \mathcal{E}_6, & \mathcal{E}_7 &= \mathcal{H}_x - \mathcal{F}_6, \\ \mathcal{F}_8 &= \mathcal{H}_q - \mathcal{E}_5, & \mathcal{E}_8 &= \mathcal{H}_x - \mathcal{F}_5. \end{aligned} \tag{13}$$

As expected, this change of bases results in switching the symmetry roots and the new symmetry root basis for the Laguerre recurrence is

$$\begin{aligned} \alpha_0 &= \mathcal{H}_y - \mathcal{F}_{12}, & \alpha_2 &= 2\mathcal{H}_x + \mathcal{H}_y - \mathcal{F}_{125678}, \\ \alpha_1 &= 2\mathcal{H}_x + \mathcal{H}_y - \mathcal{F}_{345678}, & \alpha_3 &= \mathcal{H}_y - \mathcal{F}_{34}, \end{aligned} \tag{14}$$

and on this root basis the translation dynamics becomes standard,

$$\tilde{\varphi}_*(\alpha) = \alpha + \langle 1, -1, -1, 1 \rangle \delta. \tag{15}$$

Note that this change of basis also acts on the surface root basis by the Dynkin diagram automorphisms, so our new surface root basis now is

$$\begin{aligned} \delta_0 &= \mathcal{F}_3 - \mathcal{F}_4, & \delta_2 &= \mathcal{H}_x - \mathcal{F}_{13}, & \delta_4 &= \mathcal{F}_6 - \mathcal{F}_7, & \delta_6 &= \mathcal{F}_5 - \mathcal{F}_6. \\ \delta_1 &= \mathcal{F}_1 - \mathcal{F}_2, & \delta_3 &= \mathcal{H}_y - \mathcal{F}_{56}, & \delta_5 &= \mathcal{F}_7 - \mathcal{F}_8, \end{aligned} \tag{16}$$

2.4 Root variables and the parameter matching

Before finding the change of coordinates that identifies the two dynamics, we need to match the Laguerre weight parameters α , s and the recurrence step n with the standard parameters, or the *root variables* a_i . Recall that the root variables are given by the *Period Map* $\chi : Q = \text{Span}_{\mathbb{Z}} \alpha_i \rightarrow \mathbb{C}$, $a_i = \chi(\alpha_i)$. To define the period map we need to find the symplectic form ω such that $-\omega = -\mathcal{K}_X$, i.e., so that the polar divisor of ω is a $(2, 2)$ -curve on $\mathbb{P}^1 \times \mathbb{P}^1$ passing through all the base points q_1, \dots, q_8 . Direct computation shows that, in the affine chart (x, y) , $\omega = (k/x^2)dx \wedge dy$. The period map computation is then based on the following facts [Sak01]:

- each symmetry root α_i can be represented (in a non-unique way) as a difference of classes of two effective divisors, $\alpha_i = [C_i^1] - [C_i^0]$;
- for each such representation there exists a unique irreducible component d_k of the anti-canonical divisor $-K_X$ such that $d_k \bullet C_i^1 = d_k \bullet C_i^0 = 1$; put $P_i = d_k \cap C_i^0$ and $Q_i = d_k \cap C_i^1$.

Then

$$\chi(\alpha_i) = \chi([C_i^1] - [C_i^0]) = \int_{P_i}^{Q_i} \frac{1}{2\pi i} \oint_{d_k} \omega = \int_{P_i}^{Q_i} \text{res}_{d_k} \omega. \quad (17)$$

In our case, the period map is given by the following Lemma.

Lemma 6.

(i) *The residues of the symplectic form ω along the irreducible components d_i of the polar divisor corresponding to the surface roots $\delta_i = [d_i]$, given in (16), are given by*

$$\begin{aligned} \text{res}_{d_0} \omega &= k dv_3, & \text{res}_{d_2} \omega &= 0, & \text{res}_{d_4} \omega &= 0, & \text{res}_{d_6} \omega &= k \frac{k}{v_5^2} dv_5. \\ \text{res}_{d_1} \omega &= k dv_1, & \text{res}_{d_3} \omega &= 0, & \text{res}_{d_5} \omega &= k dv_7, \end{aligned}$$

(ii) *For the standard root variable normalization $\chi(\delta) = a_0 + a_1 = a_1 + a_2 = 1$ we need to take $k = -1$ and the root variables a_i are then given by*

$$a_0 = -n, \quad a_1 = n + 1, \quad a_2 = 1 + n + \alpha, \quad a_3 = -(n + \alpha). \quad (18)$$

Proof. Detailed examples of such computations can be found in [DT18, DFS20], so here we only explain one such computation. Consider the root α_1 and represent it as a difference of two effective classes:

$$\alpha_1 = 2\mathcal{H}_x + \mathcal{H}_y - \mathcal{F}_3 - \mathcal{F}_4 - \mathcal{F}_5 - \mathcal{F}_6 - \mathcal{F}_7 - \mathcal{F}_8 = [2H_x + H_y - F_3 - F_4 - F_5 - F_6 - F_7] - [F_8].$$

The first class is a class of a proper transform of a $(2, 1)$ -curve passing through the points q_3, \dots, q_7 and a direct computation shows that its equation in the affine (x, y) -chart is $x(x +$

$n + \alpha) + y - s = 0$. The second class is the class of the exceptional divisor F_8 , so we need to consider these curves in the (u_7, v_7) -chart. In this chart the proper transform $2H_x + H_y - F_{34567}$ is given by the equation $v_7 - (n + \alpha) + u_7(s + (n + \alpha)v_7 - su_7v_7) = 0$, which intersects with the irreducible divisor $d_5 = F_7 - F_8$, given by the equation $u_7 = 0$, at the point $(u_7, v_7) = (0, n + \alpha)$. The exceptional divisor F_8 intersects with d_5 at the point $q_8(0, 1 + 2n + \alpha)$. Computing the symplectic form ω in the (u_7, v_7) -chart,

$$\omega = k \frac{dx \wedge dy}{x^2} = k \frac{dX \wedge dY}{Y^2} = k \frac{du_5 \wedge dv_5}{u_5 v_5^2} = k \frac{du_6 \wedge dv_6}{u_6^2 v_6^2} = k \frac{du_7 \wedge dv_7}{u_7(1 - u_7 v_7)^2},$$

we see that

$$\text{res}_{d_5} \omega = \text{res}_{u_7=0} k \frac{du_7 \wedge dv_7}{u_7(1 - u_7 v_7)^2} = k dv_7, \quad \chi(\alpha_1) = \int_{v_7=1+2n+\alpha}^{v_7=n+\alpha} k dv_7 = -k(n + 1).$$

Other computations are similar and we get

$$a_0 = kn, \quad a_1 = -k(n + 1), \quad a_2 = -k(1 + n + \alpha), \quad a_3 = k(n + \alpha).$$

The normalization $\chi(\delta) = a_0 + a_1 = a_1 + a_2 = -k = 1$ then tells us that $k = -1$. \square

Remark 7. Note that the root variable evolution under the discrete step $n \mapsto n + 1$ is given by

$$\bar{a}_0 = a_0 - 1, \quad \bar{a}_1 = a_1 + 1, \quad \bar{a}_2 = a_2 + 1, \quad \bar{a}_3 = a_3 - 1,$$

which corresponds to the correct (dual) translation on the root basis given by (15).

2.5 The change of coordinates

We are finally in the position to prove Theorem 1 that gives the explicit change of coordinates matching the dynamics (6) and (42). For that, we use the change of basis (13) in Lemma 5. This computation is standard, see [DT18, DFS20] for detailed examples, so here we only outline it. From the change of basis on the Picard lattice for the coordinate classes,

$$\mathcal{H}_q = \mathcal{H}_x, \quad \mathcal{H}_p = 2\mathcal{H}_x + \mathcal{H}_y - \mathcal{F}_5 - \mathcal{F}_6 - \mathcal{F}_7 - \mathcal{F}_8,$$

we see that, up to Möbius transformations, $q \sim x$, and p is a (projective) coordinate on a pencil $|H_p| = |2H_x + H_y - F_{5678}|$ of $(2, 1)$ -curves passing through the points q_5, q_6, q_7, q_8 , and so $p \sim x^2 + x(1 + 2n + \alpha) + y$. Thus, we take the change of coordinates to be

$$q(x, y) = \frac{Ax + B}{Cx + D}, \quad p(x, y) = \frac{K(x^2 + x(1 + 2n + \alpha) + y) + L}{M(x^2 + x(1 + 2n + \alpha) + y) + N},$$

where A, \dots, N are parameters of Möbius transformations that can be found from the knowledge of the divisor mapping, see [CDT17]. For example, from the correspondence

$F_1 - F_2 = E_3 - E_4$ we see that under the change of coordinates the point $q_1(0, 0)$ should map to the point $p_3(\infty, 0)$, i.e.,

$$Q(0, 0) = \frac{C \cdot 0 + D}{A \cdot 0 + B} = \frac{D}{B} = 0, \quad p(0, 0) = \frac{L}{N} = 0 \implies D = L = 0,$$

and then we can take $C = K = 1$ to get

$$q(x, y) = A + \frac{B}{x}, \quad p(x, y) = \frac{(x^2 + x(1 + 2n + \alpha) + y)}{M(x^2 + x(1 + 2n + \alpha) + y) + N}.$$

From the correspondence $F_7 - F_8 = E_5 - E_6$ we see that the change of coordinates mapping, when written in the charts $(u_7, v_7) \rightarrow (q, P)$ and restricted to $u_7 = 0$, should map to $(q = 0, P = 0)$:

$$q(u_7, v_7) = A + Bu_7, \\ P(u_7, v_7) = -\frac{u_7(v_7(M(\alpha + 2n + 1) + Nu_7) - N) - M(\alpha + 2n - v_7 + 1)}{\alpha - v_7(u_7(\alpha + 2n + 1) + 1) + 2n + 1},$$

so $q(0, v_7) = A = 0$ and $P(0, v_7) = M = 0$. Thus,

$$q(x, y) = \frac{B}{x}, \quad p(x, y) = \frac{(x^2 + x(1 + 2n + \alpha) + y)}{N}.$$

Proceeding in the same way, from the correspondence $F_3 - F_4 = E_1 - E_2$ we deduce that $N = s$, from the correspondence $F_4 = E_2$ we get $B(1 + n) = -sa_1$, and since we know, from the period map computation, that $a_1 = n + 1$, we get $B = -s$ which gives us the required change of variables (7). Finally, from the correspondence $F_5 - F_6 = E_7 - E_8$ we get the relationship between the weight parameter s and the Painlevé parameter t , $s = -t$. The inverse change of variables can now be either obtained directly, or computed in the similar way. This concludes the proof of Theorem 1.

2.6 Half-maps and the point evolution

Consider now the individual maps $\tilde{\varphi}_1 : (x, y) \rightarrow (x, \bar{y})$ and $\tilde{\varphi}_2 : (x, y) \mapsto (\underline{x}, y)$. Using the action of the half-maps on the Picard lattice described in Lemma 2, we see that the corresponding action on the symmetry roots α_i , given by (14), is

$$(\tilde{\varphi}_1)_* : \langle \alpha_0, \alpha_1, \alpha_2, \alpha_3 \rangle \mapsto \langle \alpha_1, \alpha_0, \alpha_3, \alpha_2 \rangle, \\ (\tilde{\varphi}_2)_* : \langle \alpha_0, \alpha_1, \alpha_2, \alpha_3 \rangle \mapsto \langle -\alpha_0, 2\alpha_0 + \alpha_1, \alpha_2 + 2\alpha_3, -\alpha_3 \rangle.$$

The standard techniques (see, e.g., [DT15]) then allow us to decompose these mappings in terms of generators of the extended affine Weyl symmetry group $\widetilde{W}(2A_1^{(1)})$ described in Section A.2. We get

$$\tilde{\varphi}_1 \sim \sigma_2 \sigma_1 \sigma_2 \sigma_1 : (x, y) \rightarrow (\tilde{x}, \tilde{y}), \quad \tilde{\varphi}_2 \sim w_0 w_3 : (x, y) \rightarrow (\underline{x}, y). \quad (19)$$

However, these mappings differ from the mappings $\tilde{\varphi}_i$ by some small gauge transformations. Specifically, $\tilde{x} = -x$, $\tilde{y} = \bar{y}$, $\tilde{x} = -x$, and $\tilde{y} = y$. For the full maps these gauge transformations cancel each other and the decomposition of, for example, the forward map is, as expected, the same as the decomposition of the standard discrete Painlevé equation [111] given in (41),

$$\begin{aligned}\tilde{\varphi} &= \tilde{\varphi}_2^{-1} \circ \tilde{\varphi}_1 = w_3 w_0 \sigma_2 \sigma_1 \sigma_2 \sigma_1 = w_3 \sigma_2 \sigma_1 \sigma_2 \sigma_1 w_1 \\ &= \sigma_2 \sigma_1 \sigma_2 \sigma_1 w_2 w_1 = \sigma_1 \sigma_2 \sigma_1 \sigma_2 w_2 w_1 : (x, y) \mapsto (\bar{x}, \bar{y}),\end{aligned}$$

where we used various commutation relations in the extended affine Weyl group $\widetilde{W}(2A_1^{(1)})$. However, these gauge transformations actually explain the evolution of points under half-maps given in Lemma 2 parts (a) and (b). For example, under the forward half-map $\tilde{\varphi}_1$ the points q_2 , q_4 , and q_8 evolve as

$$\begin{aligned}q_2(u_1 = 0, v_1 = -n = a_0) &\mapsto \tilde{q}_2(\tilde{u}_1 = -\bar{u}_1 = 0, \tilde{v}_1 = -\bar{v}_1 = -\bar{a}_0 = -a_1 = -(n+1)), \\ q_4(u_3 = 0, v_3 = -(n+\alpha) = a_3) &\mapsto \tilde{q}_4(\tilde{u}_3 = 0, \tilde{v}_3 = -\bar{v}_3 = -\bar{a}_3 = -a_2 = -(n+1+\alpha)), \\ q_8(u_7 = 0, v_7 = 1+2n+\alpha = a_2 - a_0) &\mapsto \tilde{q}_8(\tilde{u}_7 = 0, \\ &\tilde{v}_7 = -\bar{v}_7 = -\bar{a}_2 + \bar{a}_0 = a_1 - a_3 = 1+2n+\alpha),\end{aligned}$$

and so it looks like points q_2 and q_4 evolve with the parameter n , and the point q_8 remains stationary. The situation with the backward half-map $\tilde{\varphi}_2$ is similar. This somewhat delicate point is explained at length in [DFS20, Section2.9].

3 Generalized Charlier Polynomials and the alt. d-P_{II} Equation

In this section we consider another example of a recurrence relation that appeared in the study of orthogonal polynomials, this time the polynomials with the generalized Charlier weight.

Recall that, given some parameter $a > 0$, the classical Charlier polynomials $C_n(x; a)$ ([Chi78, Chapter VI], [KLS10, 9.14]) are polynomials that are orthogonal on the lattice $\mathbb{N} = \{0, 1, 2, 3, \dots\}$ with respect to the Poisson distribution:

$$\sum_{k=0}^{\infty} C_n(k; a) C_m(k; a) \frac{a^k}{k!} = a^{-n} \exp(a) n! \delta_{n,m}, \quad a > 0.$$

The three term recurrence relation for the Charlier polynomials is

$$-xC_n(x; a) = aC_{n+1}(x; a) - (n+a)C_n(x; a) + nC_{n-1}(x; a),$$

and the corresponding normalized recurrence relation for the *monic* polynomials $P_n(x; a)$ is

$$xP_n(x; a) = P_{n+1}(x; a) + b_n P_n(x; a) + a_n^2 P_{n-1}(x; a), \quad C_n(x; a) = \left(-\frac{1}{a}\right)^n P_n(x; a),$$

where the recurrence coefficients are given explicitly by $a_n^2 = na$ and $b_n = n + a$ for $n \in \mathbb{N}$. In [SVA12] the classical Charlier weight was generalized by adding one more parameter $\beta > 0$ to the weight function. The resulting function $w(x) = \frac{\Gamma(\beta)a^x}{\Gamma(\beta+x)\Gamma(x+1)}$, when restricted to the lattice \mathbb{N} , becomes $w(k) = \frac{a^k}{(\beta)_k k!}$, where $(\cdot)_k$ is the usual Pochhammer symbol. Corresponding monic orthogonal polynomials $P_n(x; a, \beta)$ satisfy

$$\sum_{k=0}^{\infty} P_n(k; a, \beta) P_m(k; a, \beta) \frac{a^k}{(\beta)_k k!} = 0, \quad n \neq m; \quad (20)$$

$$xP_n(x; a, \beta) = P_{n+1}(x; a, \beta) + b_n P_n(x; a, \beta) + a_n^2 P_{n-1}(x; a, \beta).$$

Recurrence coefficients a_n^2 and b_n are described by the following Theorem.

Theorem 8. [SVA12, Th. 2.1] *The recurrence coefficients for the orthogonal polynomials defined by (20) on the lattice \mathbb{N} satisfy*

$$b_n + b_{n-1} - n + \beta = \frac{an}{a_n^2}, \quad (21)$$

$$(a_{n+1}^2 - a)(a_n^2 - a) = a(b_n - n)(b_n - n + \beta - 1),$$

with the initial conditions

$$a_0^2 = 0, \quad b_0 = \frac{\sqrt{a}I_\beta(2\sqrt{a})}{I_{\beta-1}(2\sqrt{a})}, \quad (22)$$

where I_β is the modified Bessel function of the first kind.

These generalized Charlier polynomials were further studied in [FVA13], where it was shown that the coefficients of the three-term recurrence relation are related to solutions of the (differential) fifth Painlevé equation P_V

$$y'' = \left(\frac{1}{2y} + \frac{1}{y-1} \right) (y')^2 - \frac{y'}{t} + \frac{(y-1)^2}{t^2} \left(Ay + \frac{B}{y} \right) + \frac{Cy}{t} + \frac{Dy(y+1)}{y-1}, \quad (23)$$

where $y = y(t)$ and A, B, C, D are arbitrary complex parameters. In [FVA13], for the generalized Charlier case, these parameters were shown to be

$$A = \frac{(\beta-1)^2}{2}, \quad B = -\frac{(n+1)^2}{2}, \quad C = 2k_1, \quad D = 0, \quad (24)$$

where t is related to the weight parameter a as $a = e^t$ and k_1 is some scaling parameter. Moreover, it was shown that the recurrence (21) was related to Bäcklund transformations of P_V . However, it is well-known, and it was also pointed out in [FVA13], that for $D = 0$ the fifth Painlevé equation P_V is in fact equivalent to the third Painlevé equation P_{III} ,

$$u'' = \frac{(u')^2}{u} - \frac{u'}{z} + \frac{\tilde{\alpha}u^2 + \tilde{\beta}}{z} + \tilde{\gamma}u^3 - \frac{\tilde{\delta}}{u}, \quad (25)$$

here $u = u(z)$ and $\tilde{\alpha}, \tilde{\beta}, \tilde{\gamma}, \tilde{\delta}$ are again arbitrary complex constants. Thus, it is more natural to study the relationship between the recurrence (21) and the Bäcklund transformations of P_{III} .

In this section we do just that. By studying (21) from the geometric point of view, we show that it is equivalent to a particular composition of elementary Bäcklund transformations, known as the alt. d- P_{II} equation. We also show explicitly how to represent that recurrence as a composition of such elementary transformations, and also give an explicit change of coordinates reducing this recurrence to the standard form.

As before, we first change the notation to $x_n := a_n^2$, $y_n := b_n$ and $\alpha := a$. Thus, our main object of study is the following discrete dynamical system:

$$\begin{cases} (x_{n+1} - \alpha)(x_n - \alpha) = \alpha(y_n - n)(y_n + \beta - n - 1), \\ y_{n-1} + y_n + \beta - n = \frac{\alpha n}{x_n}. \end{cases} \quad (26)$$

The main result of this section is the following Theorem.

Theorem 9. *Recurrence (26) is equivalent to Sakai's alt. d- P_{II} equation (44) via the following explicit change of coordinates and parameter identification:*

$$\begin{cases} x(f, g) = \frac{s(f+1-b_0)}{g}, \\ y(f, g) = f+g, \\ n = b_0 - 1, \quad \alpha = -s, \quad \beta = a_0, \end{cases} \quad \begin{cases} f(x, y) = \frac{xy - \alpha n}{x - \alpha}, \\ g(x, y) = \frac{\alpha(n-y)}{x - \alpha}, \\ a_0 = \beta, \quad b_1 = -n, \quad s = -\alpha. \end{cases} \quad (27)$$

Note that the evolution $n \rightarrow n+1$ corresponds to the correct root variables evolution $\bar{a}_0 = a_0$, $\bar{a}_1 = a_1$, $\bar{b}_0 = b_0 + 1$, $\bar{b}_1 = b_1 - 1$ (recall that $a_0 + a_1 = b_0 + b_1 = 1$).

The techniques used to establish this result are the same as in Section 2 and so here we only give a brief summary.

3.1 Identification with alt. d- P_{II} equation

Recurrence (26) defines two half-step maps, $\tilde{\psi}_1^n : (x_n, y_n) \rightarrow (x_{n+1}, y_n)$ and $\tilde{\psi}_2^n : (x_n, y_n) \rightarrow (x_n, y_{n-1})$. As usual, we put $x := x_n$, $\bar{x} := x_{n+1}$, $\underline{x} := x_{n-1}$, and similarly for y . We can then define the forward map $\tilde{\psi} := (\tilde{\psi}_2^{n+1})^{-1} \circ \tilde{\psi}_1^n : (x, y) \rightarrow (\bar{x}, \bar{y})$ and the backward map $\tilde{\psi}^{-1} := (\tilde{\psi}_1^{n-1})^{-1} \circ \tilde{\psi}_2^n : (x, y) \rightarrow (\underline{x}, \underline{y})$. These are the maps we study.

Standard computation shows that the base points of the maps $\tilde{\psi}$ and $\tilde{\psi}^{-1}$ are

$$\begin{aligned} z_1(x = \alpha, y = n), \quad z_2(x = \alpha, y = n + 1 - \beta), \\ z_3(x = 0, Y = 0) \leftarrow z_4(U_3 = xy = \alpha n, V_3 = Y = 0), \\ z_5(X = 0, Y = 0) \leftarrow z_6(U_5 = Xy = 0, V_5 = Y = 0) \leftarrow z_7(U_6 = Xy^2 = -1, V_6 = 0) \\ \leftarrow z_8(U_7 = Xy^3 + y = \beta - n, V_7 = Y = 0), \end{aligned} \quad (28)$$

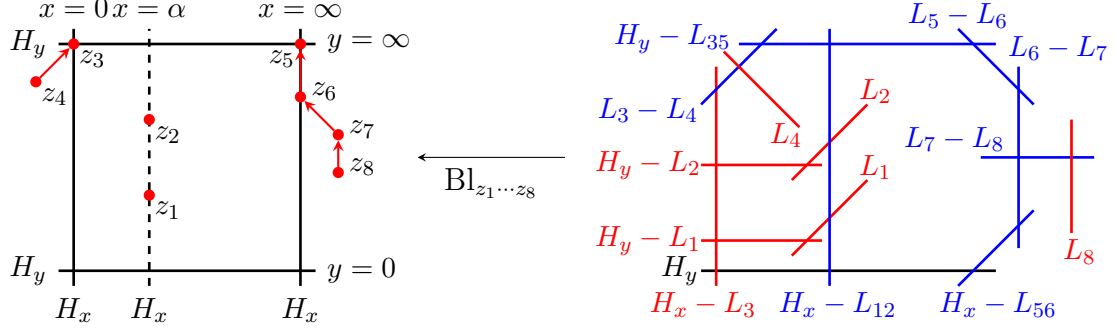


Figure 3: The Sakai Surface for the generalized Charlier recurrence

and their configuration and the resulting surface are shown on Figure 3.

We then immediately see that we get a $D_6^{(1)}$ Sakai surface, with the surface root basis shown on Figure 4.

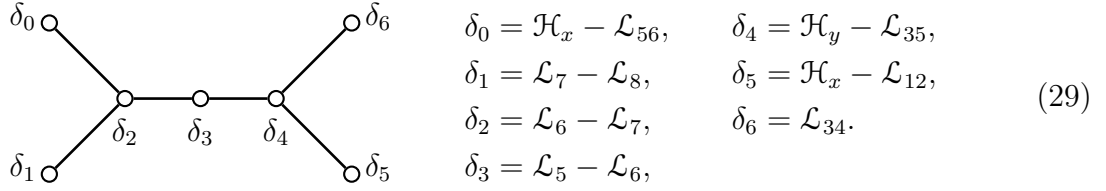


Figure 4: The Surface Root Basis for the generalized Charlier recurrence

The surface root basis (29) corresponds to the change of basis between the Sakai surface on Figure 3 and the alt. d- P_{II} surface on Figure 8 given by

$$\begin{aligned}
 \mathcal{H}_x &= \mathcal{H}_f + \mathcal{H}_g - \mathcal{K}_{16}, & \mathcal{H}_f &= \mathcal{H}_x + \mathcal{H}_y - \mathcal{L}_{13}, \\
 \mathcal{H}_y &= \mathcal{H}_f + \mathcal{H}_g - \mathcal{K}_{67}, & \mathcal{H}_g &= \mathcal{H}_x + \mathcal{H}_y - \mathcal{L}_{15}, \\
 \mathcal{L}_1 &= \mathcal{H}_f + \mathcal{H}_g - \mathcal{K}_{167}, & \mathcal{K}_1 &= \mathcal{H}_y - \mathcal{L}_1, \\
 \mathcal{L}_2 &= \mathcal{K}_8, & \mathcal{K}_2 &= \mathcal{L}_6, \\
 \mathcal{L}_3 &= \mathcal{H}_g - \mathcal{K}_6, & \mathcal{K}_3 &= \mathcal{L}_7, \\
 \mathcal{L}_4 &= \mathcal{K}_5, & \mathcal{K}_4 &= \mathcal{L}_8, \\
 \mathcal{L}_5 &= \mathcal{H}_f - \mathcal{K}_6, & \mathcal{K}_5 &= \mathcal{L}_4, \\
 \mathcal{L}_6 &= \mathcal{K}_2, & \mathcal{K}_6 &= \mathcal{H}_x + \mathcal{H}_y - \mathcal{L}_{135}, \\
 \mathcal{L}_7 &= \mathcal{K}_3, & \mathcal{K}_7 &= \mathcal{H}_x - \mathcal{L}_1, \\
 \mathcal{L}_8 &= \mathcal{K}_4, & \mathcal{K}_8 &= \mathcal{L}_2.
 \end{aligned} \tag{30}$$

Then the symmetry roots are given by

$$\begin{aligned}
 \alpha_0 &= 2\mathcal{H}_x + 2\mathcal{H}_y - 2\mathcal{L}_1 - \mathcal{L}_{345678}, & \alpha_2 &= \mathcal{H}_x + 2\mathcal{H}_y - \mathcal{L}_{125678}, \\
 \alpha_1 &= \mathcal{L}_1 - \mathcal{L}_2, & \alpha_3 &= \mathcal{H}_x - \mathcal{L}_{34}.
 \end{aligned} \tag{31}$$

The map $\tilde{\psi}$ induces the evolution $\tilde{\psi}_* : \text{Pic}(\mathcal{X}) \rightarrow \text{Pic}(\bar{\mathcal{X}})$ given by

$$\begin{aligned}
\mathcal{H}_x &\mapsto 3\bar{\mathcal{H}}_x + 2\bar{\mathcal{H}}_y - \bar{\mathcal{L}}_{12} - 2\bar{\mathcal{L}}_{34} - \bar{\mathcal{L}}_{56}, & \mathcal{L}_4 &\mapsto \bar{\mathcal{L}}_8, \\
\mathcal{H}_y &\mapsto \bar{\mathcal{H}}_x + \bar{\mathcal{H}}_y - \bar{\mathcal{L}}_{34}, & \mathcal{L}_5 &\mapsto \bar{\mathcal{H}}_x + \bar{\mathcal{H}}_y - \bar{\mathcal{L}}_{346}, \\
\mathcal{L}_1 &\mapsto \bar{\mathcal{H}}_x + \bar{\mathcal{H}}_y - \bar{\mathcal{L}}_{234}, & \mathcal{L}_6 &\mapsto \bar{\mathcal{H}}_x + \bar{\mathcal{H}}_y - \bar{\mathcal{L}}_{345}, \\
\mathcal{L}_2 &\mapsto \bar{\mathcal{H}}_x + \bar{\mathcal{H}}_y - \bar{\mathcal{L}}_{134}, & \mathcal{L}_7 &\mapsto \bar{\mathcal{H}}_x - \bar{\mathcal{L}}_4, \\
\mathcal{L}_3 &\mapsto \bar{\mathcal{L}}_7, & \mathcal{L}_8 &\mapsto \bar{\mathcal{H}}_x - \bar{\mathcal{L}}_3,
\end{aligned} \tag{32}$$

which then gives the translation

$$\tilde{\psi}_* : \boldsymbol{\alpha} = \langle \alpha_0, \alpha_1, \alpha_2, \alpha_3 \rangle \mapsto \tilde{\psi}_*(\boldsymbol{\alpha}) = \boldsymbol{\alpha} + \langle 0, 0, -1, 1 \rangle \delta \tag{33}$$

on the symmetry root lattice. Thus, we see that the dynamics is equivalent to that of the alt. d- P_{II} equation, and to prove Theorem 9 it remains to find the change of variables inducing the change of basis (30), which is done in the usual way.

4 Conclusions

In this paper we illustrated the effectiveness of the algorithmic approach, recently proposed in [DFS20], for solving the discrete Painlevé identification problem using the algebro-geometric tools of Sakai's geometric theory of Painlevé equations. We also showed how two non-equivalent standard discrete Painlevé dynamics appear in natural applied problems.

A very interesting problem is to construct a natural degeneration scheme for weights for orthogonal polynomial ensembles that corresponds to the degeneration cascade for Sakai's classification scheme for discrete Painlevé equations. The examples we considered in this paper show that any such scheme has to be more refined than just a geometric classification, and it should indeed include the class of translation elements. It is interesting and important to collect more examples of this type to better understand how such problem can be approached.

Acknowledgements

XL and DJZ are supported by the NSF of China (No. 11631007, 11875040) and Science and Technology Innovation Plan of Shanghai (No. 20590742900) from Science and Technology Commission of Shanghai Municipality. GF acknowledges the support of the National Science Center (Poland) grant OPUS 2017/25/B/BST1/00931.

A Discrete Painlevé Equations in the d-P $(2A_1^{(1)}/D_6^{(1)})$ Family

Let us very briefly recall some main ingredients of Sakai’s classification scheme [Sak01] for discrete Painlevé equations. Each such equation describes a discrete dynamical system on a certain family of rational algebraic surfaces obtained by blowing up eight points, called the *base points*, on $\mathbb{P}_{\mathbb{C}}^1 \times \mathbb{P}_{\mathbb{C}}^1$. For each family, the configuration of these base points is constrained to stay on a collection of irreducible rational (except for the elliptic case) curves – these curves are the irreducible components of the (unique) anti-canonical divisor $-K_X$ that is fixed for each family. Modulo gauging, the locations of the base points within that configuration are the parameters for the family; there exist canonical such parameters known as the *root variables*. It turns out that the intersection configuration of these irreducible components is described by some *affine Dynkin diagram* \mathcal{D}_1 (in our case, $D_6^{(1)}$) and the type of this diagram is known as the *geometric type* of the family. Symmetries of this family of surfaces form an affine Weyl group defined by some other Dynkin diagram \mathcal{D}_2 (in our case, $2A_1^{(1)}$) further extended by some diagram automorphisms. The type of the diagram \mathcal{D}_2 is known as the *symmetry type* of the family. The dynamics itself is generated by some composition of elementary symmetries and corresponds to a translation element in extended affine Weyl group $\widetilde{W}(\mathcal{D}_2)$. The conjugacy class of that element is then the type of our discrete Painlevé equation, it is a complete invariant.

Thus, we see that for each surface there are infinitely many non-equivalent discrete Painlevé dynamics. Moreover, each equation has many different coordinate realizations, since there are different ways to define point configurations of the given geometric type \mathcal{D}_1 . The standard and most studied examples of discrete Painlevé equations correspond to some particularly simple point configurations and “short” translations. Recent comprehensive survey paper [KNY17] gave standard examples of such configurations for each type, together with natural degenerations, and we use it as our main reference.

For the d-P $(2A_1^{(1)}/D_6^{(1)})$ family, the standard example in [KNY17] is equation (8.29) in Section 8.1.20. Based on the action of this dynamics on the root variables we label it as $[1\overline{1}\overline{1}1]$. However, there is also another well-known and non-equivalent example of discrete Painlevé equation of this type, known as alt. d-P_{II}, in [Sak01]. We use a slightly different form of this equation as given by equations (2.35) (2.36) in [Sak07] and label it as $[001\overline{1}]$. In this appendix we describe the point configurations for both of these equations (and fix some minor typos in [KNY17]).

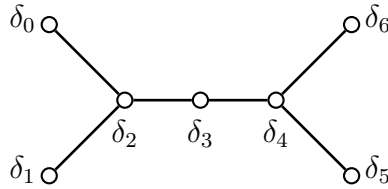
Remark 10. To see that equations $[1\overline{1}\overline{1}1]$ and $[001\overline{1}]$ are indeed non-equivalent one can, for example, compute the length of the corresponding translation vectors on the lattice. But probably the simplest way is to look at the Jordan block structure of the induced linear map on the Picard lattice. For equation $[1\overline{1}\overline{1}1]$ it is $J(-1, 1)^{\oplus 2} \oplus J(1, 1)^{\oplus 5} \oplus J(1, 3)$ and for equation $[001\overline{1}]$ it is $J(-1, 1)^{\oplus 3} \oplus J(1, 1)^{\oplus 4} \oplus J(1, 3)$.

A.1 The point configuration

Recall that the Picard lattice of a rational algebraic surface \mathcal{X} obtained by blowing up $\mathbb{P}_{\mathbb{C}}^1 \times \mathbb{P}_{\mathbb{C}}^1$ at eight points is generated by the classes of coordinate lines \mathcal{H}_1 and \mathcal{H}_2 and the classes \mathcal{E}_i of the central fibers of the blowup,

$$\text{Pic}_{\mathcal{X}} = \text{Span}_{\mathbb{Z}}\{\mathcal{H}_1, \mathcal{H}_2, \mathcal{E}_1, \dots, \mathcal{E}_8\}.$$

This lattice is equipped with the symmetric bilinear product (*intersection form*) defined on the generators by $\mathcal{H}_1 \bullet \mathcal{H}_2 = 1$, $\mathcal{H}_1 \bullet \mathcal{H}_1 = \mathcal{H}_2 \bullet \mathcal{H}_2 = \mathcal{H}_i \bullet \mathcal{E}_j = 0$, and $\mathcal{E}_i \bullet \mathcal{E}_j = -\delta_{ij}$. In this lattice we have the anti-canonical divisor class $\mathcal{K}_{\mathcal{X}} = 2\mathcal{H}_1 + 2\mathcal{H}_2 - \mathcal{E}_1 - \dots - \mathcal{E}_8$ which for the $D_6^{(1)}$ -type surface should decompose in the irreducible -2 components as $\mathcal{K}_{\mathcal{X}} = \delta = \delta_0 + \delta_1 + 2\delta_2 + 2\delta_3 + 2\delta_4 + \delta_5 + \delta_6$. In [KNY17] this decomposition is achieved by the choice of the *surface root basis* $R = \{\delta_i\}$ shown on Figure 5.



$$\begin{aligned} \delta_0 &= \mathcal{E}_1 - \mathcal{E}_2, & \delta_4 &= \mathcal{E}_6 - \mathcal{E}_7, \\ \delta_1 &= \mathcal{E}_3 - \mathcal{E}_4, & \delta_5 &= \mathcal{E}_5 - \mathcal{E}_6, \\ \delta_2 &= \mathcal{H}_1 - \mathcal{E}_{13}, & \delta_6 &= \mathcal{E}_7 - \mathcal{E}_8, \\ \delta_3 &= \mathcal{H}_2 - \mathcal{E}_{56}, \end{aligned} \tag{34}$$

Figure 5: The Surface Root Basis for the standard d-P $(2A_1^{(1)}/D_6^{(1)})$ point configuration

Let us now describe the corresponding point configuration. Take (q, p) to be the coordinates in the $\mathbb{C} \times \mathbb{C}$ affine chart and let $Q = 1/q$ and $P = 1/p$ be the coordinates at infinity. Looking at the surface root basis, we see that there are two points p_1 and p_3 on the vertical line that we can, using the Möbius group action on coordinates, take to be $q = \infty$ (or $Q = 0$). There are also two degeneration cascades (infinitely close points) $p_2 \rightarrow p_1$ and $p_4 \rightarrow p_3$. There is also a longer degeneration cascade $p_8 \rightarrow p_7 \rightarrow p_6 \rightarrow p_5$. Using Möbius group action again, we can arrange the points to be $p_1(\infty, 1)$, $p_3(\infty, 0)$, $p_5(0, \infty)$, and the only remaining gauge action is the rescaling in the q -coordinate (that we later use to normalize the root variables). We then get the point configuration shown on Figure 6. Note that one reason for choosing this point normalization is that they are located on the polar divisor of the standard symplectic form $\omega = dp \wedge dq$.

The parameterization of this point configuration in terms of root variables a_0, \dots, a_3 normalized by $a_0 + a_1 = a_2 + a_3 = 1$ is given in [KNY17],

$$p_{12} : \left(\frac{1}{\varepsilon}, 1 - a_1 \varepsilon \right)_2, \quad p_{34} : \left(\frac{1}{\varepsilon}, -a_2 \varepsilon \right)_2, \quad p_{5678} : \left(\varepsilon, -\frac{t}{\varepsilon^2} + \frac{1 - a_1 - a_2}{\varepsilon} \right)_4,$$

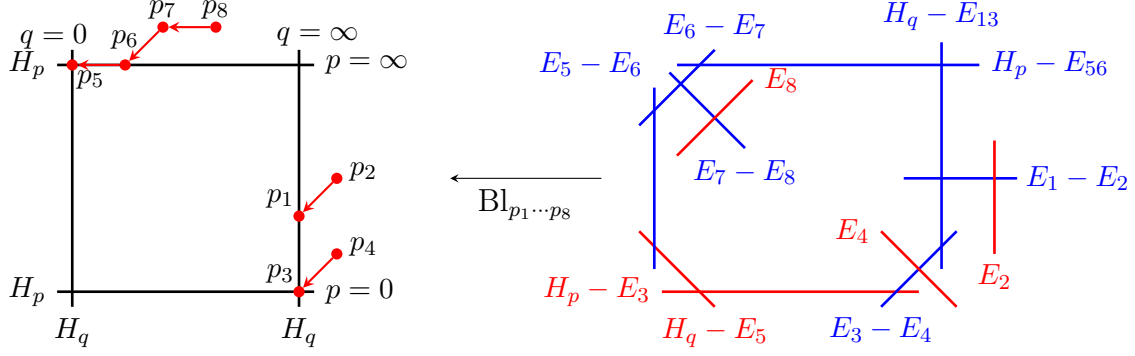


Figure 6: The model Sakai Surface for the d-P($2A_1^{(1)}/D_6^{(1)}$) example

or, explicitly,

$$\begin{aligned}
p_1(Q = 0, p = 1) &\leftarrow p_2(u_1 = Q = 0, v_1 = q(p - 1) = -a_1), \\
p_3(Q = 0, p = 0) &\leftarrow p_4(u_3 = Q = 0, v_3 = qp = -a_2), \\
p_5(q = 0, P = 0) &\leftarrow p_6(u_5 = q = 0, v_5 = PQ = 0) \leftarrow p_7 \left(u_6 = q = 0, v_6 = \frac{1}{q^2 p} = -\frac{1}{t} \right) \\
&\leftarrow p_8 \left(u_7 = q = 0, v_7 = \frac{q^2 p + t}{q^3 p t} = \frac{a_1 + a_2 - 1}{t^2} \right).
\end{aligned} \tag{35}$$

The parameter t that appears in the p_5 cascade is related to the independent variable of the differential Painlevé equation P_{III} for which this surface family, after we remove the polar divisor, is the Okamoto space of initial conditions.

A.2 The extended affine Weyl symmetry group

Consider now the symmetry root basis $R^\perp = \{\alpha_j\}$ where the symmetry roots α_j should satisfy the condition $\delta_i \bullet \alpha_j = 0$. We get a reducible affine Dynkin diagram of type $2A_1^{(1)}$ (here $\mathcal{E}_{i\dots j} = \mathcal{E}_i + \dots + \mathcal{E}_j$),

$$\begin{array}{ccc}
\begin{array}{c} \text{---} \text{---} \\ \alpha_0 \quad \alpha_1 \\ \text{---} \text{---} \\ \alpha_2 \quad \alpha_3 \end{array} & \begin{array}{l} \alpha_0 = 2\mathcal{H}_q + \mathcal{H}_p - \mathcal{E}_{345678}, \\ \alpha_2 = \mathcal{H}_p - \mathcal{E}_3 - \mathcal{E}_4, \\ -\mathcal{K}_\chi = \delta = \alpha_0 + \alpha_1 = a_2 + \alpha_3. \end{array} & \begin{array}{l} \alpha_1 = \mathcal{H}_p - \mathcal{E}_1 - \mathcal{E}_2, \\ \alpha_3 = 2\mathcal{H}_q + \mathcal{H}_p - \mathcal{E}_{125678}. \end{array} \end{array} \tag{36}$$

Figure 7: The Symmetry Root Basis for the standard d-P ($2A_1^{(1)}/D_6^{(1)}$) point configuration

The symmetry sub-lattice is $Q = \text{Span}_{\mathbb{Z}}\{R^\perp\} = \text{Span}_{\mathbb{Z}}\{\alpha_j\}$, and the root variables a_i are defined using the *Period Map* $\chi : Q \rightarrow \mathbb{C}$, $a_i = \chi(\alpha_i)$, together with the normalization

$\chi(\delta) = a_0 + a_1 = a_2 + a_3 = 1$, see example of detailed computation of the Period Map in [DT18, DFS20].

The affine Weyl group $W(2A_1^{(1)})$ is defined in terms of generators $w_i = w_{\alpha_i}$ and relations that are encoded by the affine Dynkin diagram $2A_1^{(1)}$,

$$W(2A_1^{(1)}) = W \left(\begin{array}{cc} \circ & \circ \\ \alpha_0 & \alpha_1 \\ \circ & \circ \\ \alpha_2 & \alpha_3 \end{array} \right) = \left\langle w_0, \dots, w_3 \mid w_i^2 = e, \quad w_i \circ w_j = w_j \circ w_i \text{ when } \overset{\circ}{\alpha}_i \overset{\circ}{\alpha}_j \right\rangle.$$

This group is realized via actions on $\text{Pic}(\mathcal{X})$ given by reflections in the roots α_i ,

$$w_i(\mathcal{C}) = w_{\alpha_i}(\mathcal{C}) = \mathcal{C} - 2 \frac{\mathcal{C} \bullet \alpha_i}{\alpha_i \bullet \alpha_i} \alpha_i = \mathcal{C} + (\mathcal{C} \bullet \alpha_i) \alpha_i, \quad \mathcal{C} \in \text{Pic}(\mathcal{X}). \quad (37)$$

Next we need to extend this group by the automorphisms of the Dynkin diagram (that corresponds to some re-labeling of the symmetry/surface roots) $\text{Aut}(2A_1^{(1)}) \simeq \text{Aut}(D_6^{(1)}) \simeq \mathbb{D}_4$, where \mathbb{D}_4 is the usual dihedral group of the symmetries of a square. Generators of $\text{Aut}(2A_1^{(1)})$ can be realized as compositions of reflections in some other roots in $\text{Pic}(\mathcal{X})$. We take as generators

$$\sigma_1 = w_{\varepsilon_1 - \varepsilon_3} \circ w_{\varepsilon_2 - \varepsilon_4}, \quad \sigma_2 = w_{\varepsilon_1 - \varepsilon_7} \circ w_{\varepsilon_2 - \varepsilon_8} \circ w_{\varepsilon_3 - \varepsilon_5} \circ w_{\varepsilon_4 - \varepsilon_6} \circ w_{\mathcal{H}_q - \varepsilon_5 - \varepsilon_6} \circ w_{\mathcal{H}_q - \varepsilon_3 - \varepsilon_4}$$

that permute the surface and the symmetry roots as follows (here we use the standard cycle notation for permutations): $\sigma_1 = (\alpha_0 \alpha_3)(\alpha_1 \alpha_2) = (\delta_0 \delta_1)$, $\sigma_2 = (\alpha_0 \alpha_1) = (\delta_0 \delta_6)(\delta_1 \delta_5)(\delta_2 \delta_4)$. The resulting group $\widetilde{W}(2A_1^{(1)}) = \text{Aut}(2A_1^{(1)}) \times W(2A_1^{(1)})$ is called an extended affine Weyl symmetry group and its action on $\text{Pic}(\mathcal{X})$ can be further extended to an action on point configurations by elementary birational maps (which lifts to isomorphisms $w_i : \mathcal{X}_{\mathbf{b}} \rightarrow \mathcal{X}_{\overline{\mathbf{b}}}$ on the family of Sakai's surfaces), this is known as a *birational representation*. We describe it in the following Lemma.

Lemma 11. *The action of the generators of the extended affine Weyl group $\widetilde{W}(2A_1^{(1)})$ on some initial point configuration*

$$\begin{pmatrix} a_0 & a_1; & t; & q, p \\ a_2 & a_3 \end{pmatrix}$$

described using the root variables in the affine (q, p) chart is given by the following birational

maps:

$$\begin{aligned}
w_0 &: \left(\begin{array}{cc} -a_0 & 2a_0 + a_1 \\ a_2 & a_3 \end{array}; t; \left(\frac{1}{q} - \frac{a_0}{q^2 p + a_2 q + t} \right)^{-1}, \right. \\
&\quad \left. \left(p - \frac{a_0(qp + a_2)}{q^2 p + a_2 q + t} \right) \left(1 - \frac{a_0 q}{q^2 p + a_2 q + t} \right) \right), \\
w_1 &: \left(\begin{array}{cc} a_0 + 2a_1 & -a_1 \\ a_2 & a_3 \end{array}; t; q + \frac{a_1}{p-1}, p \right), \\
w_2 &: \left(\begin{array}{cc} a_0 & a_1 \\ -a_2 & 2a_2 + a_3 \end{array}; t; q + \frac{a_2}{p}, p \right), \\
w_3 &: \left(\begin{array}{cc} a_0 & a_1 \\ a_2 + 2a_3 & -a_3 \end{array}; t; \frac{q(\Upsilon + a_3 q)}{\Upsilon}, 1 + \frac{\Upsilon((p-1)\Upsilon - a_1 a_3)}{(\Upsilon + a_3 q)^2} \right),
\end{aligned}$$

where $\Upsilon = q^2(p-1) + (a_1 - a_3)q + t$,

$$\begin{aligned}
\sigma_1 &: \left(\begin{array}{cc} a_3 & a_2 \\ a_1 & a_0 \end{array}; -t; -q, 1-p \right), \\
\sigma_2 &: \left(\begin{array}{cc} a_1 & a_0 \\ a_2 & a_3 \end{array}; t; \frac{t}{q}, -\frac{q(qp + a_2)}{t} \right).
\end{aligned}$$

The proof is standard, see [DFS20, DT18] for similar computations explained in detail. Note that although expressions for w_0 and w_3 look quite complicated, they can be represented in terms of simpler generators as $w_0 = \sigma_2 w_1 \sigma_2$, $w_3 = \sigma_1 w_0 \sigma_1 = \sigma_1 \sigma_2 w_1 \sigma_2 \sigma_1$.

A.3 Discrete Painlevé equations on the $D_6^{(1)}$ surface

There are two natural simple examples.

A.3.1 The $[\overline{1111}]$ Discrete Painlevé Equation

One standard reference example of a discrete Painlevé equation on the $D_6^{(1)}$ surface is given in [KNY17]* as

$$\bar{q} + q = -\frac{a_2}{p} - \frac{a_1}{p-1}, \quad p + \underline{p} = 1 + \frac{1 - a_2 - a_1}{q} - \frac{t}{q^2}, \quad (38)$$

with the root variables evolution and normalization as follows

$$\bar{a}_0 = a_0 - 1, \quad \bar{a}_1 = a_1 + 1, \quad \bar{a}_2 = a_2 + 1, \quad \bar{a}_3 = a_3 - 1, \quad a_0 + a_1 = a_2 + a_3 = 1. \quad (39)$$

*In [KNY17, Equations (8.29–8.30)] a_2 should in fact be a_0 and an additional normalization $a_2 + a_3 = 1$ is missing.

From the evolution of the root variables (39) we can immediately see that the corresponding translation on the root lattice is

$$\varphi_* : \alpha = \langle \alpha_0, \alpha_1, \alpha_2, \alpha_3 \rangle \mapsto \varphi_*(\alpha) = \alpha + \langle 1, -1, -1, 1 \rangle \delta, \quad (40)$$

and that is why we denote this equation by $[1\bar{1}\bar{1}1]$. The decomposition of the Painlevé map φ can be written using the generators of $\widehat{W}(2A_1^{(1)})$ as (see [DT18] on detailed explanation on how to obtain such decompositions)

$$\varphi = \sigma_1 \sigma_2 \sigma_1 \sigma_2 w_2 w_1 = \varphi_2^{-1} \circ \varphi_1, \quad (41)$$

where partial mappings $\varphi_1 = w_2 w_1 : (q, p) \rightarrow (-\bar{q}, p)$ and $\varphi_2 = \sigma_2 \sigma_1 \sigma_2 \sigma_1 : (q, p) \rightarrow (-q, \underline{p})$ correspond, up to some gauge transformation, to half maps given in (38) (see [DFS20, Section 2.9] for detailed explanations about such gauge ambiguities). The full map then is

$$\varphi \left(\begin{matrix} a_0 & a_1 \\ a_2 & a_3 \end{matrix}; t; q, p \right) = \left(\begin{matrix} a_0 - 1 & a_1 + 1 \\ a_2 + 1 & a_3 - 1 \end{matrix}; t; \begin{matrix} \bar{q} = -q - \frac{a_2}{p} - \frac{a_1}{p-1}, \\ \bar{p} = 1 - p + \frac{1 - \bar{a}_1 - \bar{a}_2}{\bar{q}} - \frac{t}{\bar{q}^2} \end{matrix} \right). \quad (42)$$

Note that the evolution (42) induces the evolution $\varphi_* : \text{Pic}(\mathcal{X}) \rightarrow \text{Pic}(\bar{\mathcal{X}})$ given by

$$\begin{aligned} \mathcal{H}_q &\mapsto 5\bar{\mathcal{H}}_q + 2\bar{\mathcal{H}}_p - \bar{\mathcal{E}}_{1234} - 2\bar{\mathcal{E}}_{5678}, & \mathcal{E}_4 &\mapsto 2\bar{\mathcal{H}}_q + \bar{\mathcal{H}}_p - \bar{\mathcal{E}}_{15678}, \\ \mathcal{H}_p &\mapsto 2\bar{\mathcal{H}}_q + \bar{\mathcal{H}}_p - \bar{\mathcal{E}}_{5678}, & \mathcal{E}_5 &\mapsto \bar{\mathcal{H}}_q - \bar{\mathcal{E}}_8, \\ \mathcal{E}_1 &\mapsto 2\bar{\mathcal{H}}_q + \bar{\mathcal{H}}_p - \bar{\mathcal{E}}_{45678}, & \mathcal{E}_6 &\mapsto \bar{\mathcal{H}}_q - \bar{\mathcal{E}}_7, \\ \mathcal{E}_2 &\mapsto 2\bar{\mathcal{H}}_q + \bar{\mathcal{H}}_p - \bar{\mathcal{E}}_{35678}, & \mathcal{E}_7 &\mapsto \bar{\mathcal{H}}_q - \bar{\mathcal{E}}_6, \\ \mathcal{E}_3 &\mapsto 2\bar{\mathcal{H}}_q + \bar{\mathcal{H}}_p - \bar{\mathcal{E}}_{25678}, & \mathcal{E}_8 &\mapsto \bar{\mathcal{H}}_q - \bar{\mathcal{E}}_5, \end{aligned} \quad (43)$$

which gives the expected translation (40) on the symmetry root lattice.

A.3.2 The $[00\bar{1}1]$ Discrete Painlevé Equation

A different version of a simple discrete Painlevé equation on the $D_6^{(1)}$ surface was given in [Sak01], where this equation was called *alt. d- P_{II}* equation[†]. A slightly different version of the equation was given in [Sak07, Equations (2.35–2.36)], this is the version we consider. We can think about this equation as a birational map given in affine coordinates (f, g) by

$$\psi \left(\begin{matrix} a_0 & a_1 \\ b_0 & b_1 \end{matrix}; s; f, g \right) = \left(\begin{matrix} a_0 & a_1 \\ b_0 + 1 & b_1 - 1 \end{matrix}; s; \bar{f} = b_0 - a_0 - f - g - \frac{s}{g}, \bar{g} = \frac{s}{g} - \frac{b_0 s}{g\bar{f}} \right), \quad (44)$$

where parameters a_i and b_i are again the root variables normalized by $a_0 + a_1 = b_0 + b_1 = 1$. In fact, parameters b_0 and b_1 correspond to parameters a_2 and a_3 in (42), and so the corresponding translation on the symmetry root lattice is

$$\psi_* : \alpha = \langle \alpha_0, \alpha_1, \alpha_2, \alpha_3 \rangle \mapsto \psi_*(\alpha) = \alpha + \langle 0, 0, -1, 1 \rangle \delta, \quad (45)$$

[†]Some minor typos were later corrected in [Sak07, Remark 2.2].

and that is why we denote this equation by $[00\bar{1}1]$. To see this we need to look at the geometry of this mapping, which is quite different from our model surface on Figure 6. The base points are

$$\begin{aligned}
\pi_1(f = b_0 - 1, g = 0), \\
\pi_2(F = 0, g = 0) &\leftarrow \pi_3(u_2 = F = 0, v_2 = fg = -s) \\
&\leftarrow \pi_4(u_3 = F = 0, v_3 = f(fg + s) = a_0s), \\
\pi_5(f = 0, G = 0), \\
\pi_6(F = 0, G = 0) &\leftarrow \pi_7(u_6 = F = 0, v_6 = fG = -1) \\
&\leftarrow \pi_8(u_7 = F = 0, v_7 = f(1 + fG) = a_0 - b_0),
\end{aligned} \tag{46}$$

(where as usual $F = 1/f$, $G = 1/g$) and their configuration and the resulting surface are shown on Figure 8.

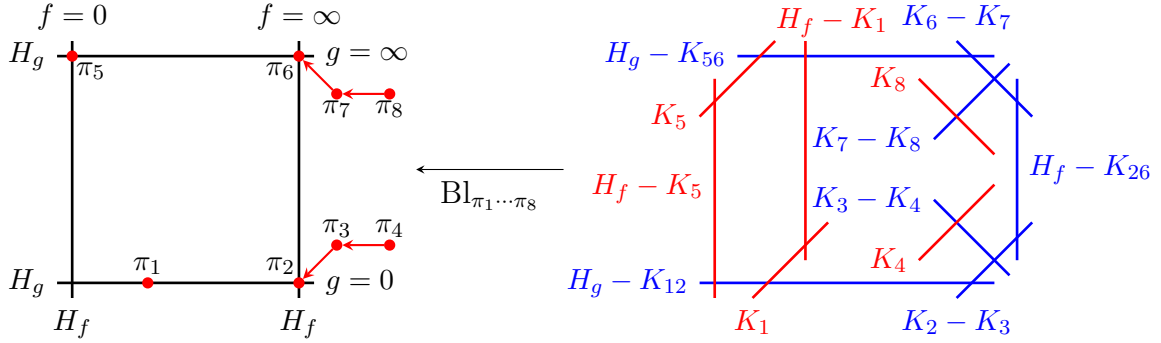


Figure 8: The Sakai Surface for the alt. $d\text{-}P_{\text{II}}$ equation

Lemma 12. *On the level of the Picard lattice the basis identification between the model $d\text{-}P(2A_1^{(1)}/D_6^{(1)})$ surface on Figure 6 and the surface for the alt. $d\text{-}P_{\text{II}}$ equation on Figure 8 is given by*

$$\begin{aligned}
\mathcal{H}_f &= 2\mathcal{H}_q + \mathcal{H}_p - \mathcal{E}_{1567}, & \mathcal{H}_q &= \mathcal{H}_g, \\
\mathcal{H}_g &= \mathcal{H}_q, & \mathcal{H}_p &= \mathcal{H}_f + 2\mathcal{H}_g - \mathcal{K}_{2678}, \\
\mathcal{K}_1 &= \mathcal{E}_2, & \mathcal{E}_1 &= \mathcal{H}_g - \mathcal{K}_2, \\
\mathcal{K}_2 &= \mathcal{H}_q - \mathcal{E}_1, & \mathcal{E}_2 &= \mathcal{K}_1, \\
\mathcal{K}_3 &= \mathcal{E}_3, & \mathcal{E}_3 &= \mathcal{K}_3, \\
\mathcal{K}_4 &= \mathcal{E}_4, & \mathcal{E}_4 &= \mathcal{K}_4, \\
\mathcal{K}_5 &= \mathcal{E}_8, & \mathcal{E}_5 &= \mathcal{H}_g - \mathcal{K}_8, \\
\mathcal{K}_6 &= \mathcal{H}_q - \mathcal{E}_7, & \mathcal{E}_6 &= \mathcal{H}_g - \mathcal{K}_7, \\
\mathcal{K}_7 &= \mathcal{H}_q - \mathcal{E}_6, & \mathcal{E}_7 &= \mathcal{H}_g - \mathcal{K}_6, \\
\mathcal{K}_8 &= \mathcal{H}_q - \mathcal{E}_5, & \mathcal{E}_8 &= \mathcal{K}_5.
\end{aligned} \tag{47}$$

This gives the following identification between the surface and the symmetry root bases:

$$\begin{aligned}
\delta_0 = \mathcal{E}_1 - \mathcal{E}_2 &= \mathcal{H}_g - \mathcal{K}_{12}, \\
\delta_1 = \mathcal{E}_3 - \mathcal{E}_4 &= \mathcal{K}_3 - \mathcal{K}_4, \\
\delta_2 = \mathcal{H}_q - \mathcal{E}_{13} &= \mathcal{K}_2 - \mathcal{K}_3, \\
\delta_3 = \mathcal{H}_p - \mathcal{E}_{56} &= \mathcal{H}_f - \mathcal{K}_{26}, \\
\delta_4 = \mathcal{E}_6 - \mathcal{E}_7 &= \mathcal{K}_6 - \mathcal{K}_7, \\
\delta_5 = \mathcal{E}_5 - \mathcal{E}_6 &= \mathcal{K}_7 - \mathcal{K}_8, \\
\delta_6 = \mathcal{E}_7 - \mathcal{E}_8 &= \mathcal{H}_g - \mathcal{K}_{56}, \\
\alpha_0 = 2\mathcal{H}_q + \mathcal{H}_p - \mathcal{E}_{345678} &= \mathcal{H}_f + \mathcal{H}_g - \mathcal{K}_{2345}, \\
\alpha_1 = \mathcal{H}_p - \mathcal{E}_{12} &= \mathcal{H}_f + \mathcal{H}_g - \mathcal{K}_{1678}, \\
\alpha_2 = \mathcal{H}_p - \mathcal{E}_{34} &= \mathcal{H}_f + 2\mathcal{H}_g - \mathcal{K}_{234678}, \\
\alpha_3 = 2\mathcal{H}_q + \mathcal{H}_p - \mathcal{E}_{125678} &= \mathcal{H}_f - \mathcal{K}_{15}.
\end{aligned} \tag{48}$$

The map (44) induces the evolution $\psi_* : \text{Pic}(\mathcal{X}) \rightarrow \text{Pic}(\overline{\mathcal{X}})$ given by

$$\begin{aligned}
\mathcal{H}_f &\mapsto 3\overline{\mathcal{H}}_f + 2\overline{\mathcal{H}}_g - 2\overline{\mathcal{K}}_1 - \overline{\mathcal{K}}_{23} - 2\overline{\mathcal{K}}_5 - \overline{\mathcal{K}}_{67}, & \mathcal{K}_4 &\mapsto \overline{\mathcal{H}}_f - \overline{\mathcal{K}}_1, \\
\mathcal{H}_g &\mapsto \overline{\mathcal{H}}_f + \overline{\mathcal{H}}_g - \overline{\mathcal{K}}_{15}, & \mathcal{K}_5 &\mapsto \overline{\mathcal{K}}_4, \\
\mathcal{K}_1 &\mapsto \overline{\mathcal{K}}_8, & \mathcal{K}_6 &\mapsto \overline{\mathcal{H}}_f + \overline{\mathcal{H}}_g - \overline{\mathcal{K}}_{135}, \\
\mathcal{K}_2 &\mapsto \overline{\mathcal{H}}_f + \overline{\mathcal{H}}_g - \overline{\mathcal{K}}_{157}, & \mathcal{K}_7 &\mapsto \overline{\mathcal{H}}_f + \overline{\mathcal{H}}_g - \overline{\mathcal{K}}_{125}, \\
\mathcal{K}_3 &\mapsto \overline{\mathcal{H}}_f + \overline{\mathcal{H}}_g - \overline{\mathcal{K}}_{156}, & \mathcal{K}_8 &\mapsto \overline{\mathcal{H}}_f - \overline{\mathcal{K}}_5,
\end{aligned} \tag{49}$$

which gives the expected translation (45) on the symmetry root lattice.

Finally, the change of variables and parameter correspondence between these two models is given by

$$\left\{ \begin{array}{l} f(q, p) = q(p-1) - \frac{s}{q} + b_0 - a_0, \\ g(q, p) = \frac{s}{q}, \\ s = -t, \quad b_0 = a_2, \quad b_1 = a_3, \end{array} \right. \quad \text{and conversely,} \quad \left\{ \begin{array}{l} q(f, g) = -\frac{t}{g}, \\ p(f, g) = 1 - \frac{g}{t}(f + g + a_0 - a_2), \\ t = -s, \quad a_2 = b_0, \quad a_3 = b_1. \end{array} \right. \tag{50}$$

The proof of this Lemma is standard and is omitted.

Remark 13. Note that alt. d-P_{II} map ψ can be written using the generators of $\widetilde{W}(2A_1^{(1)})$ as $\psi = \sigma_1 \sigma_2 \sigma_1 w_2$ and the corresponding mapping in the standard model is given by

$$\psi \left(\begin{array}{cc} a_0 & a_1 \\ a_2 & a_3 \end{array}; t; q, p \right) = \left(\begin{array}{cc} a_0 & a_1 \\ a_2 + 1 & a_3 - 1 \end{array}; s; \bar{q} = -\frac{pt}{pq + a_2}, \bar{p} = \frac{\bar{q}(\bar{q} - a_1) + t(p-1)}{\bar{q}^2} \right). \tag{51}$$

References

- [AB06] D. Arinkin and A. Borodin, *Moduli spaces of d-connections and difference Painlevé equations*, Duke Math. J. **134** (2006), no. 3, 515–556.
- [AB09] D Arinkin and A. Borodin, *Tau-function of discrete isomonodromy transformations and probability*, Compos. Math. **145** (2009), no. 3., 747–772

- [BB03] Alexei Borodin and Dmitriy Boyarchenko, *Distribution of the first particle in discrete orthogonal polynomial ensembles*, Comm. Math. Phys. **234** (2003), no. 2, 287–338.
- [Bor03] Alexei Borodin, *Discrete gap probabilities and discrete Painlevé equations*, Duke Math. J. **117** (2003), no. 3, 489–542.
- [CC15] Min Chen and Yang Chen, *Singular linear statistics of the Laguerre unitary ensemble and Painlevé III. Double scaling analysis*, J. Math. Phys. **56** (2015), no. 6, 063506, 14.
- [CDT17] Adrian Stefan Carstea, Anton Dzhamay, and Tomoyuki Takenawa, *Fiber-dependent deautonomization of integrable 2D mappings and discrete Painlevé equations*, J. Phys. A **50** (2017), no. 40, 405202, 41.
- [CFR19] Yang Chen, Galina Filipuk, and Maria das Neves Rebocho, *Nonlinear difference equations for a modified Laguerre weight: Laguerre-Freud equations and asymptotics*, Jaen J. Approx. **11** (2019), no. 1-2, 47–65.
- [Chi78] T. S. Chihara, *An introduction to orthogonal polynomials*, Gordon and Breach Science Publishers, New York-London-Paris, 1978, Mathematics and its Applications, Vol. 13.
- [CI10] Yang Chen and Alexander Its, *Painlevé III and a singular linear statistics in Hermitian random matrix ensembles. I*, J. Approx. Theory **162** (2010), no. 2, 270–297.
- [DFS20] Anton Dzhamay, Galina Filipuk, and Alexander Stokes, *Recurrence coefficients for discrete orthogonal polynomials with hypergeometric weight and discrete Painlevé equations*, J. Phys. A: Math. Theor. **53** (2020), no. 495201, 29.
- [DT15] Anton Dzhamay and Tomoyuki Takenawa, *Geometric analysis of reductions from Schlesinger transformations to difference Painlevé equations*, Algebraic and analytic aspects of integrable systems and Painlevé equations, Contemp. Math., vol. 651, Amer. Math. Soc., Providence, RI, 2015, pp. 87–124.
- [DT18] Anton Dzhamay and Tomoyuki Takenawa, *On some applications of Sakai’s geometric theory of discrete Painlevé equations*, SIGMA Symmetry Integrability Geom. Methods Appl. **14** (2018), no. 075, 20.
- [FVA13] Galina Filipuk and Walter Van Assche, *Recurrence coefficients of generalized Charlier polynomials and the fifth Painlevé equation*, Proc. Amer. Math. Soc. **141** (2013), no. 2, 551–562.
- [GH78] Phillip Griffiths and Joseph Harris, *Principles of algebraic geometry*, Wiley-Interscience [John Wiley & Sons], New York, 1978, Pure and Applied Mathematics.

- [KLS10] Roelof Koekoek, Peter A. Lesky, and René F. Swarttouw, *Hypergeometric orthogonal polynomials and their q -analogues*, Springer Monographs in Mathematics, Springer-Verlag, Berlin, 2010, With a foreword by Tom H. Koornwinder.
- [KNY17] Kenji Kajiwara, Masatoshi Noumi, and Yasuhiko Yamada, *Geometric aspects of Painlevé equations*, J. Phys. A **50** (2017), no. 7, 073001, 164.
- [Sak01] Hidetaka Sakai, *Rational surfaces associated with affine root systems and geometry of the Painlevé equations*, Comm. Math. Phys. **220** (2001), no. 1, 165–229.
- [Sak07] ———, *Problem: discrete Painlevé equations and their Lax forms*, Algebraic, analytic and geometric aspects of complex differential equations and their deformations. Painlevé hierarchies, RIMS Kôkyûroku Bessatsu, B2, Res. Inst. Math. Sci. (RIMS), Kyoto, 2007, pp. 195–208.
- [Sha13] Igor R. Shafarevich, *Basic algebraic geometry 1*, Third ed., Springer, Heidelberg, 2013, Varieties in projective space.
- [SVA12] Christophe Smet and Walter Van Assche, *Orthogonal polynomials on a bi-lattice*, Constr. Approx. **36** (2012), no. 2, 215–242.
- [VA18] Walter Van Assche, *Orthogonal polynomials and Painlevé equations*, Australian Mathematical Society Lecture Series, vol. 27, Cambridge University Press, Cambridge, 2018.
- [XDZ15] Shuai-Xia Xu, Dan Dai, and Yu-Qiu Zhao, *Painlevé III asymptotics of Hankel determinants for a singularly perturbed Laguerre weight*, J. Approx. Theory **192** (2015), 1–18.